# NANOTECHNOLOGY IN HIGH LASER FIELDS (ON THE WAY TOWARDS NUCLEAR FUSION)

NORBERT KROO
WIGNER RESEARCH CENTER OF PHYSICS and
HUNGARIAN ACADEMY OF SCIENCES

***Motto: Only those, who are prepared to go too far, can know how far they may go.***

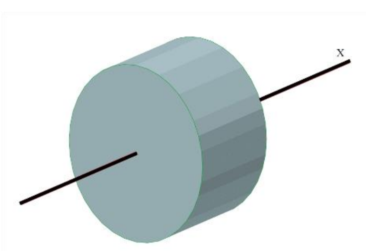


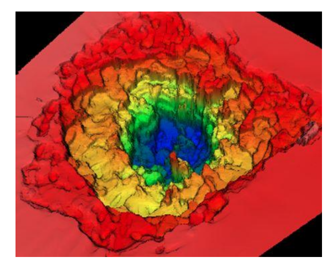

SZEGED, ELI-ALPS 2023.10.19

# Matter under extreme conditions

## (extremely high intensities)

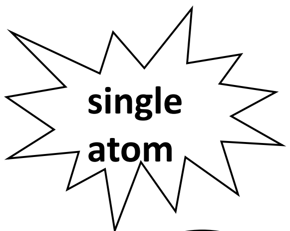


$I = 10^{16}$ W cm$^{-2}$ → E ~ $10^{9}$ V/cm

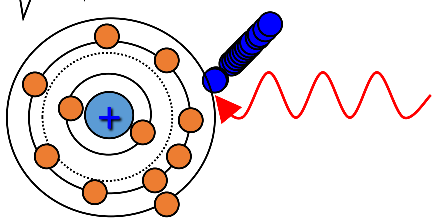

High intensity
Photoeletric Effect

*Rapid ionization of valence electrons*

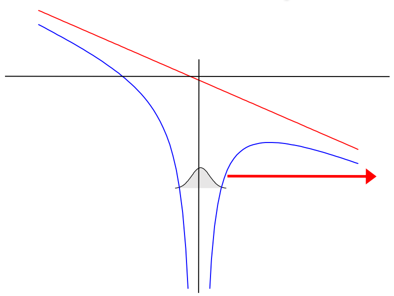

$$V = -\frac{q}{x} \pm E.x$$

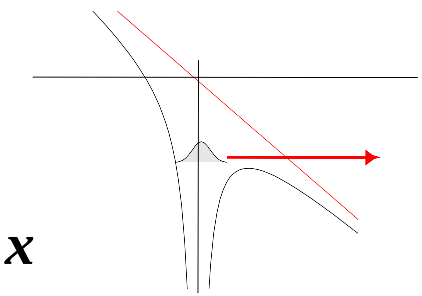

Tunnelling

$10^{14}$ - $10^{15}$ W cm$^{-2}$

Over the barrier

> $10^{15}$ W cm$^{-2}$

Each atom loses at least one electron. Some can lose as many as 6 !

# MULTIPHOTON ELECTRON EMISSION FROM GOLD

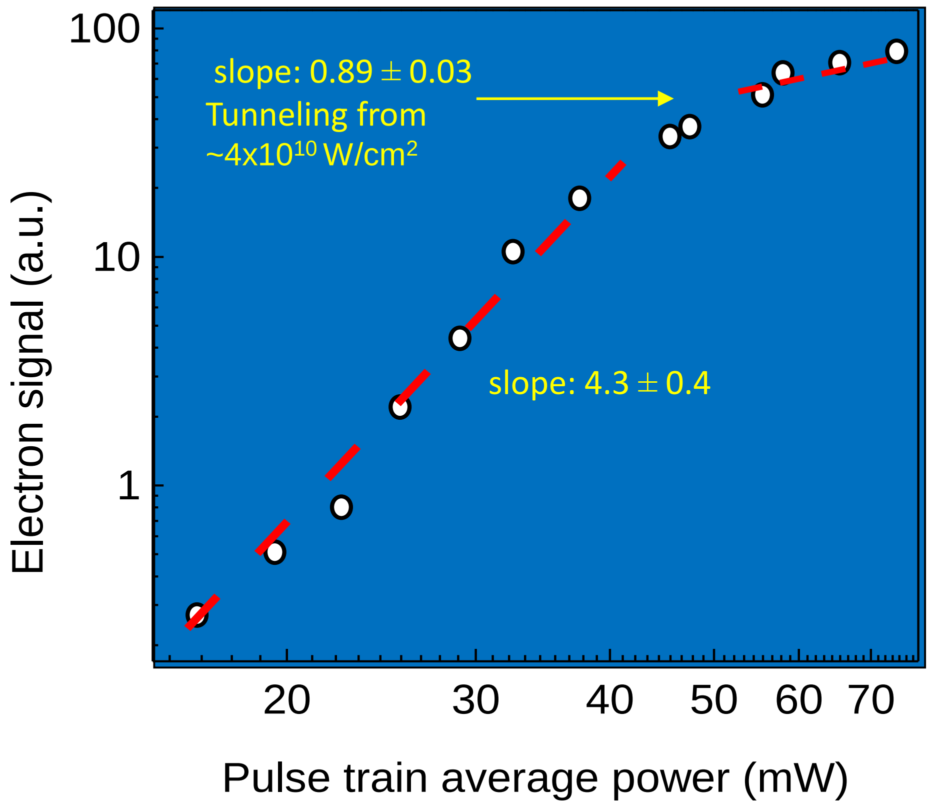


Multiphoton → tunneling transition at ~$4\times10^{10}$ W/cm$^2$ incident intensity, ~$5.5\times10^{8}$ V/m field

Keldysh-gamma $\gamma$=31

→ indication of well-known field enhancement of surface plasmonic fields

**PLASMONIC ENHANCEMENT!**

$$\gamma^2 = \frac{W}{2U_p} = \left(\frac{\omega\sqrt{2mW}}{eE_l}\right)^2$$

*W*: work function, $E_l$: laser field strength

# SURFACE PLASMONS AND THEIR PROPAGATION

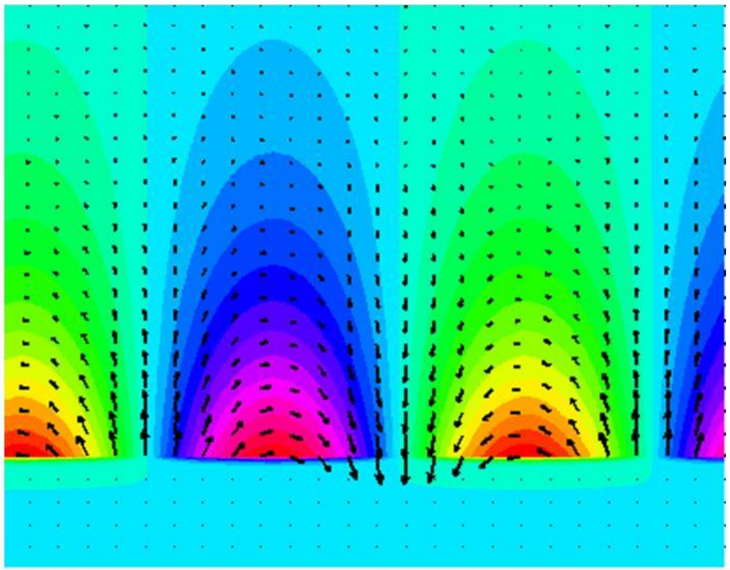

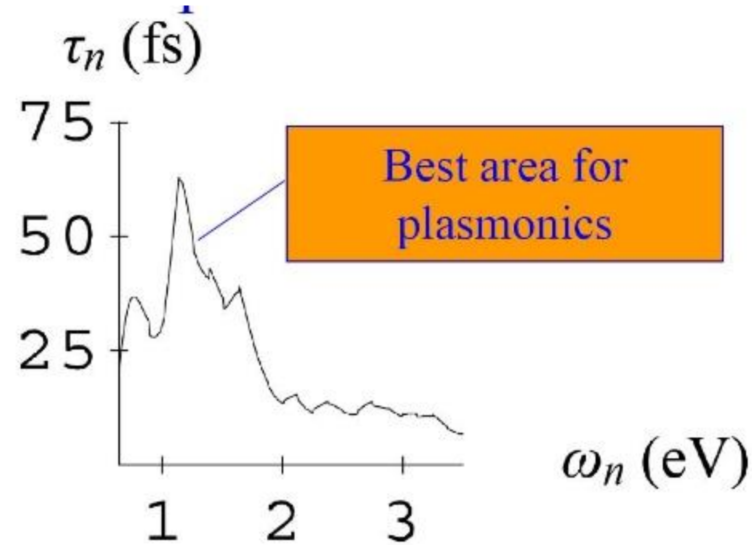


$\varepsilon = \varepsilon_1 + i.\varepsilon_2 \quad \varepsilon_1<0$

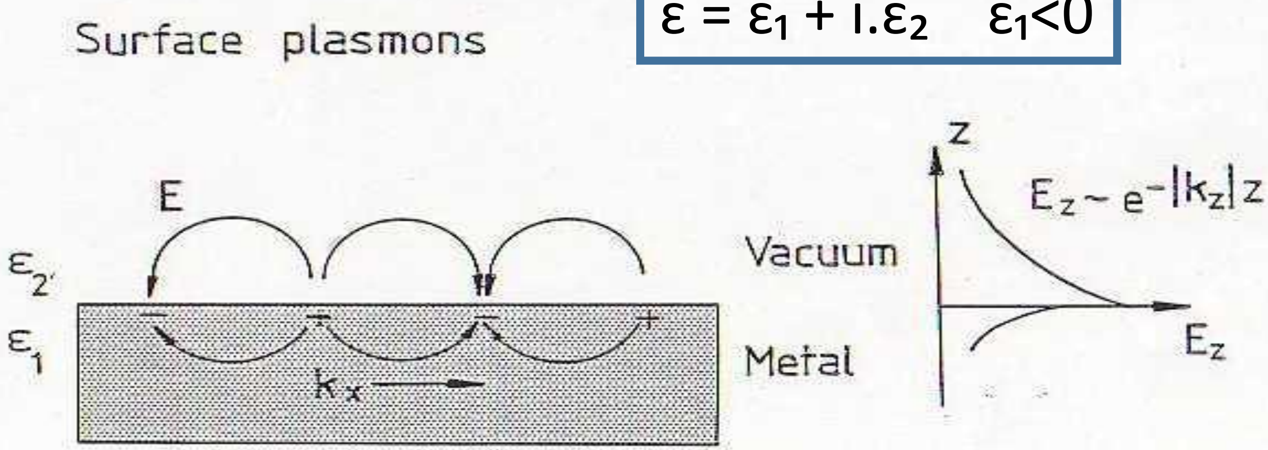


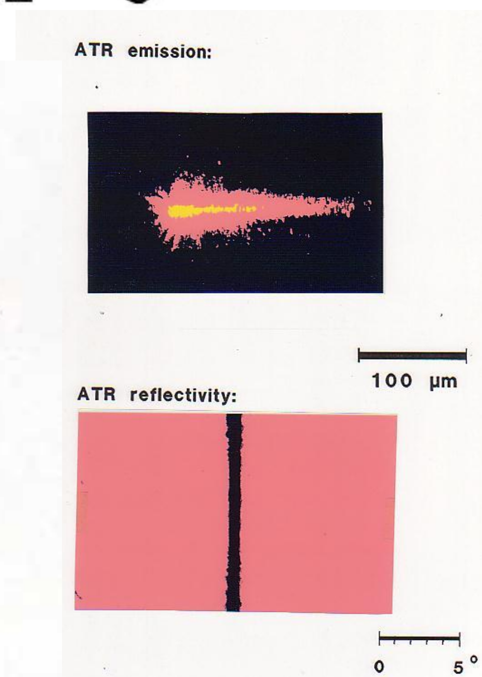

# LOCALIZED SURFACE PLASMON POLARITONS

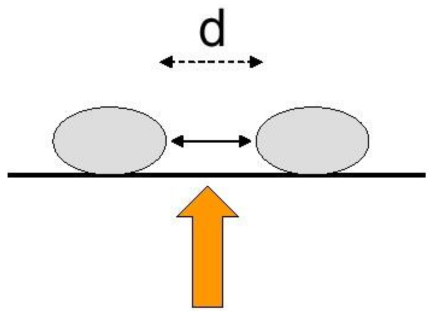


**d << λ**

"Near-field coupling"

⇒ Resonator coupling

**d >> λ**

"Dipole-dipole coupling"

⇒ Interferences

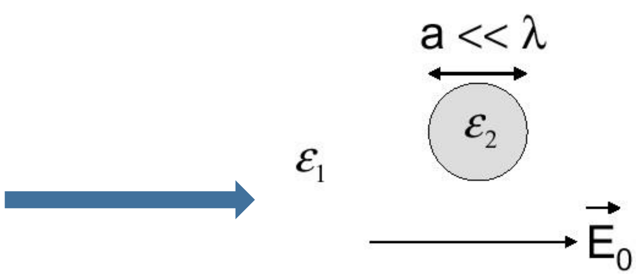


If a << λ ⇒ dipole :

$$p = \varepsilon_2 \, \alpha \, E_0$$

with:

$$\alpha = 4\pi \, a^3 \frac{\varepsilon_2 - \varepsilon_1}{\varepsilon_2 + 2\varepsilon_1}$$

**HOT SPOTS!**

Resonance when $\varepsilon_2\ (\omega) = -\ 2 \times \varepsilon_1\ (\omega)$

- Enhanced absorption
- Enhancement of the near-field & scattering

# LOCALIZED PLASMONS (LSPP, UP TO $10^{20}$ W/cm² proved)

(The basic difference between SPP-s and LSPP-s)

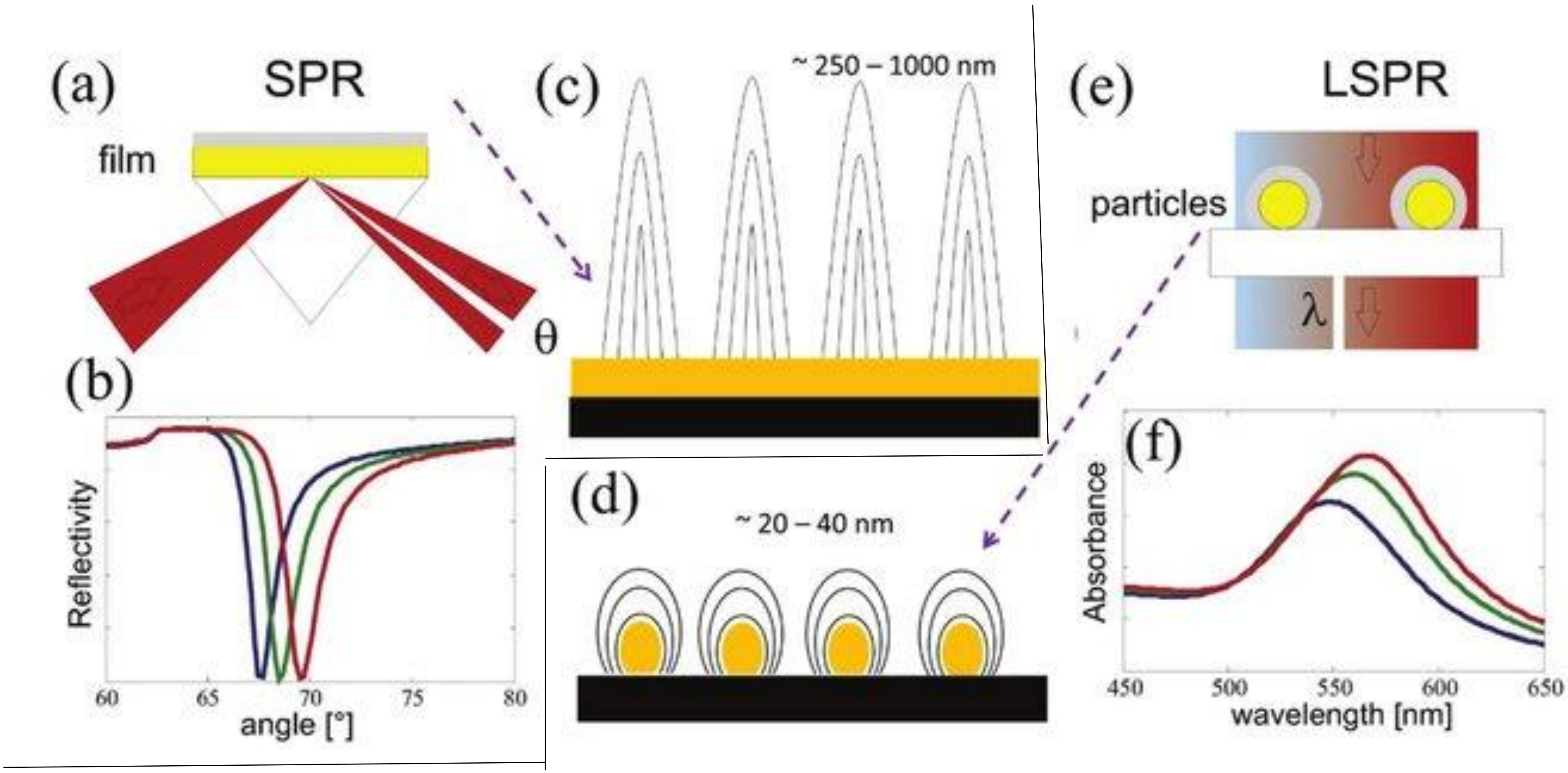


LSPP: - NO PENETRATION INTO THE PLASMONIC MATERIAL (e.g. metal)
- SMALLER PENETRATION DISTANCE INTO THE DIELECTRIC /VACUUM
- NO DISPERSION
- BROADER RESONANCE

# Nanorod:Transverse and longitudinal modes!

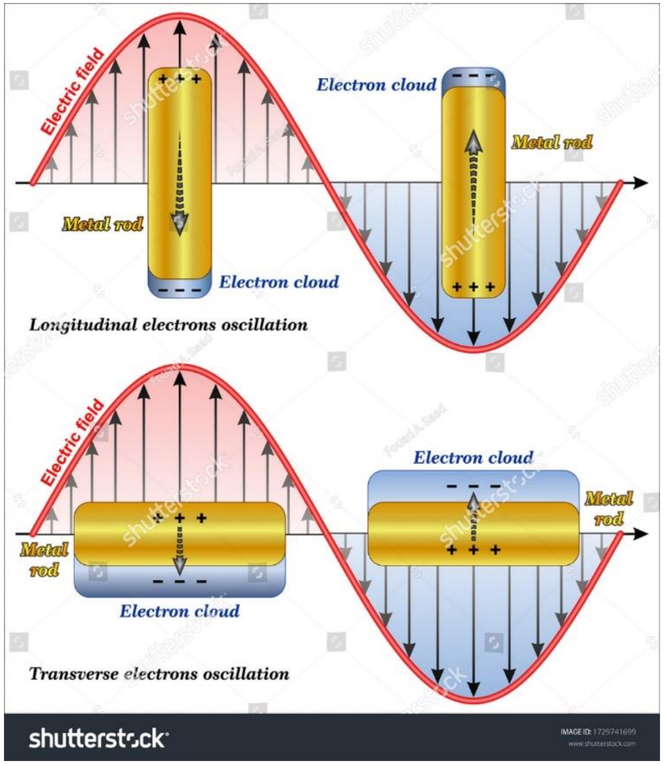


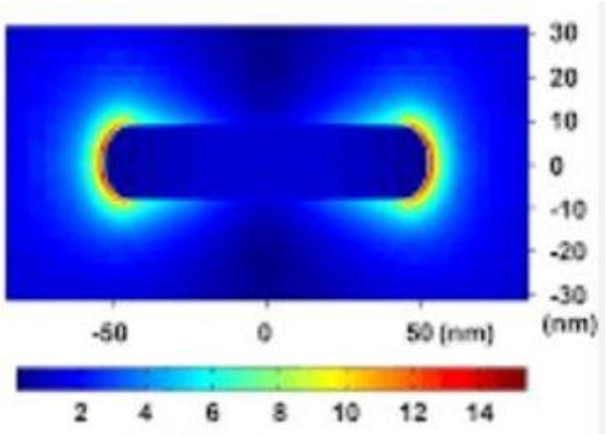


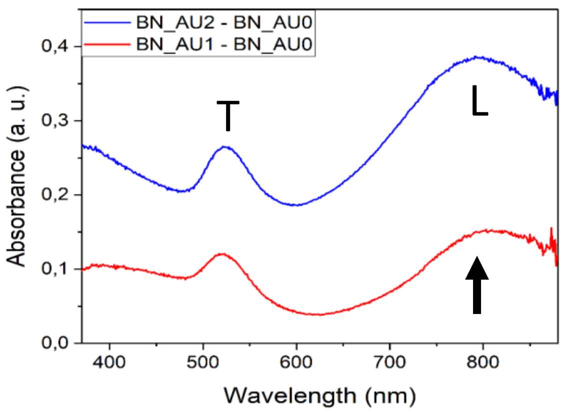


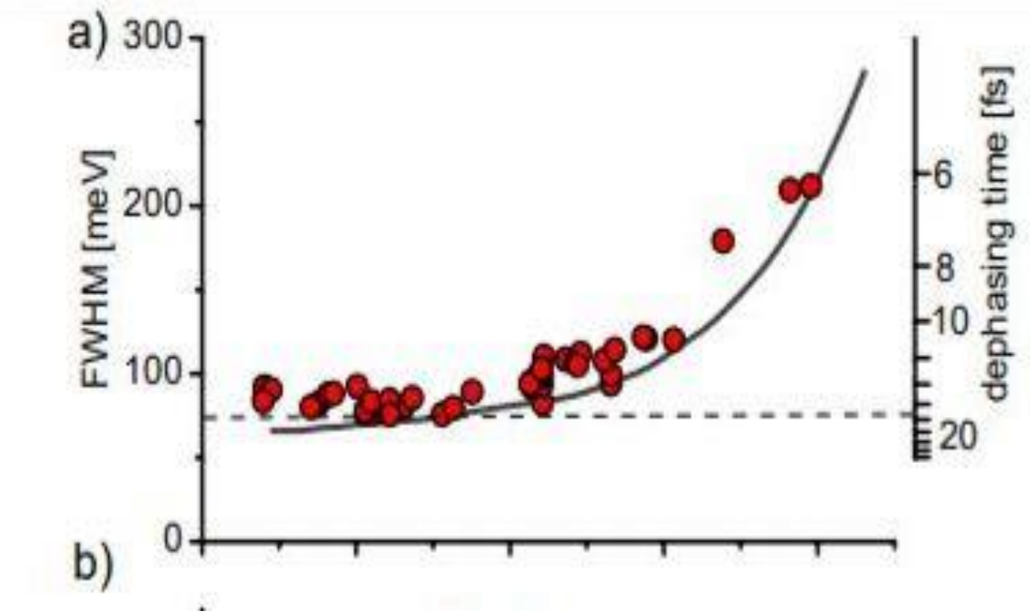

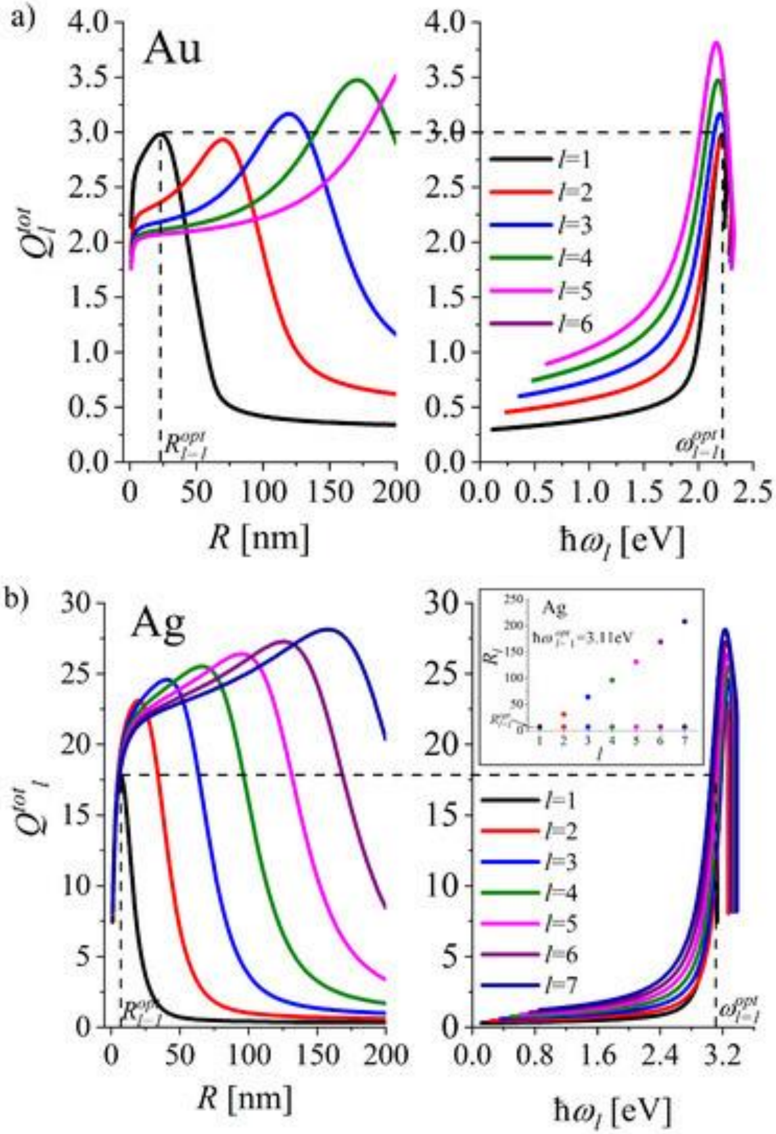


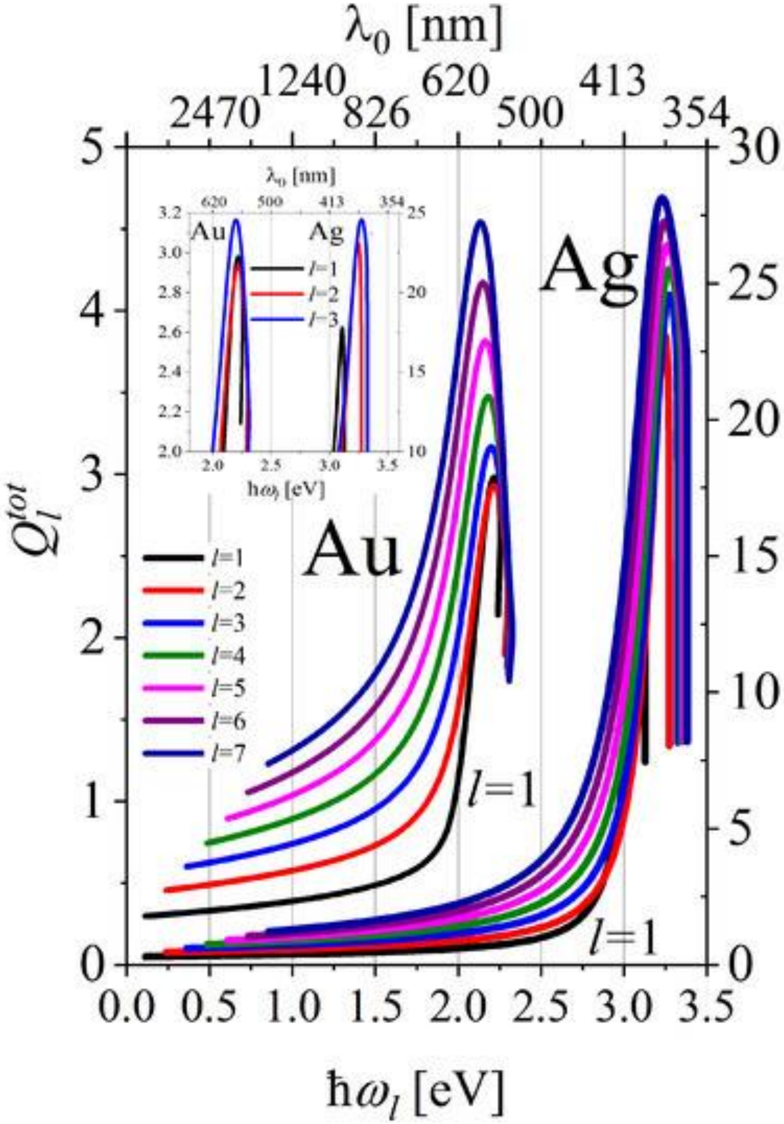


Krystina Kolwas: Materials 2023, 16,1801, pp1-15

# Some potential new energy technologies

## (involving nanotechnologies)

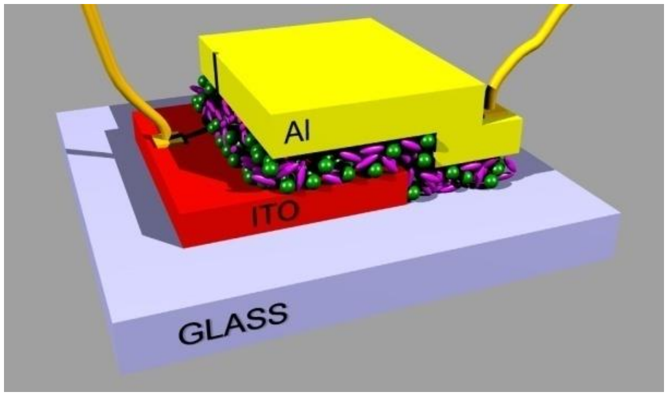


**P3HT Cell**
**efficiency = 6%**
**SPESC (P3HT)**
**efficiency = 17.5%**

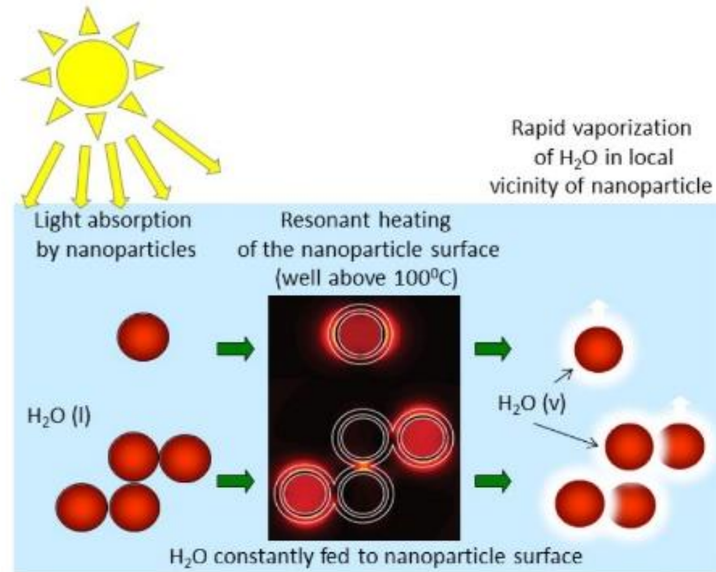


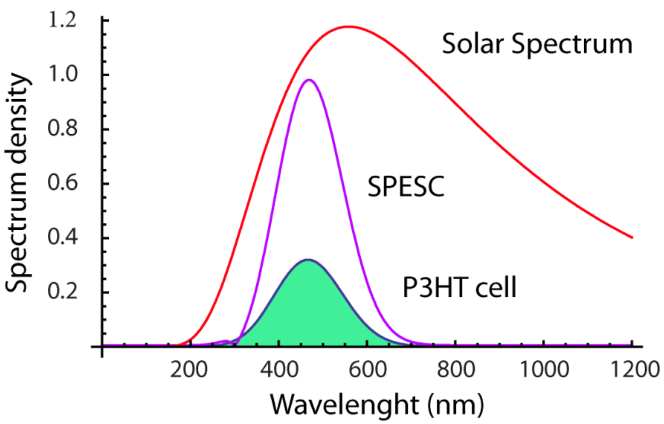


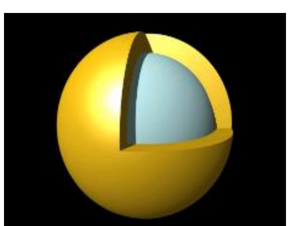

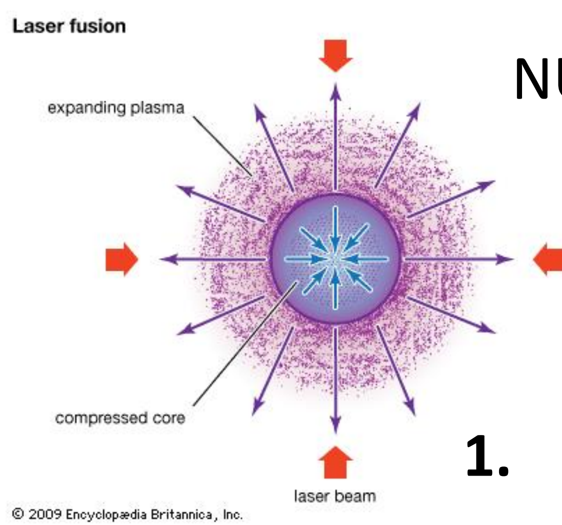


HIGH FIELDS.
NUCLEAR FUSION

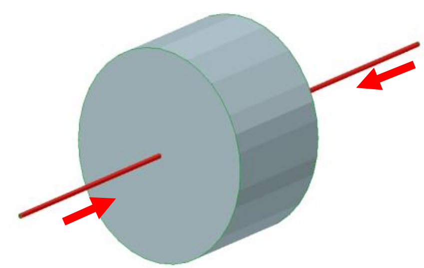

**1.** Toward our proposal **2.**

# THE MAGNETIC CONFINEMENT FUSION REACTOR (ITER): (inside view)

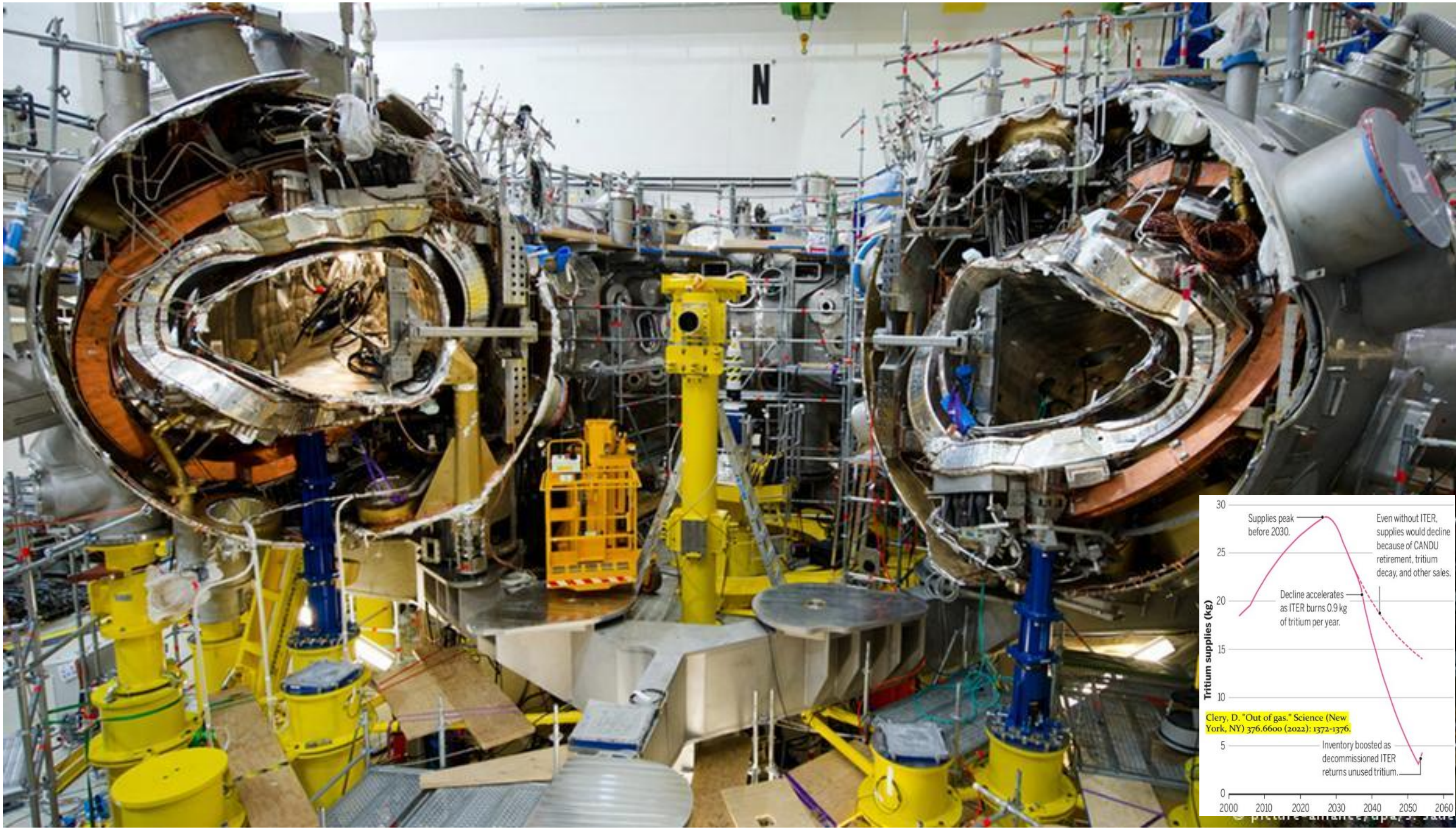


Problems: costs; size; tritium supply (?); construction materials; delay; etc.

# No1. application (NIF)

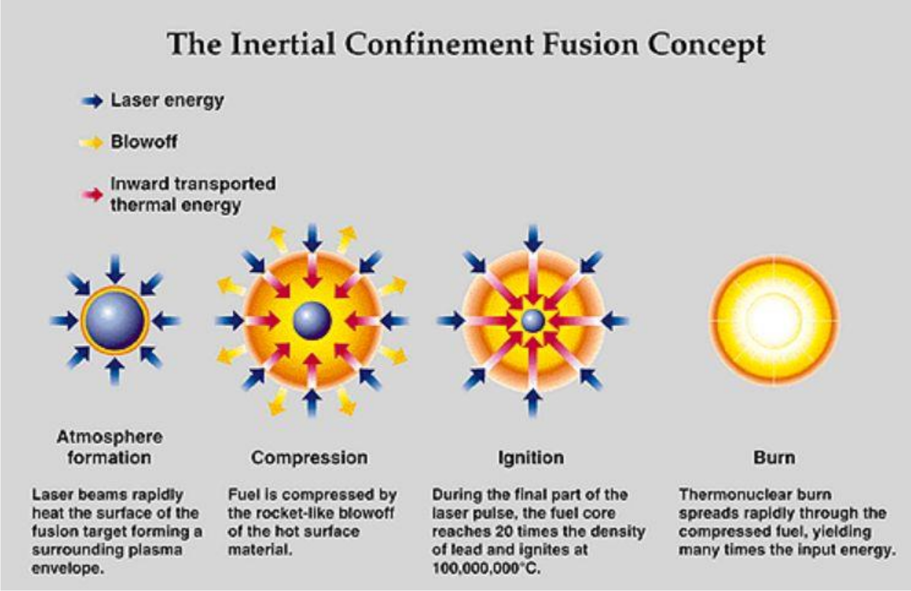


The most succesful technologies imitate nature

$E = mc^2$

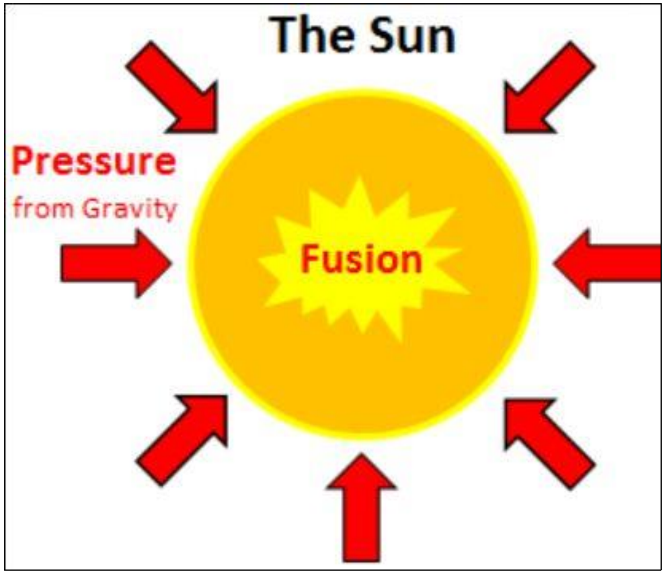


Laserbeams

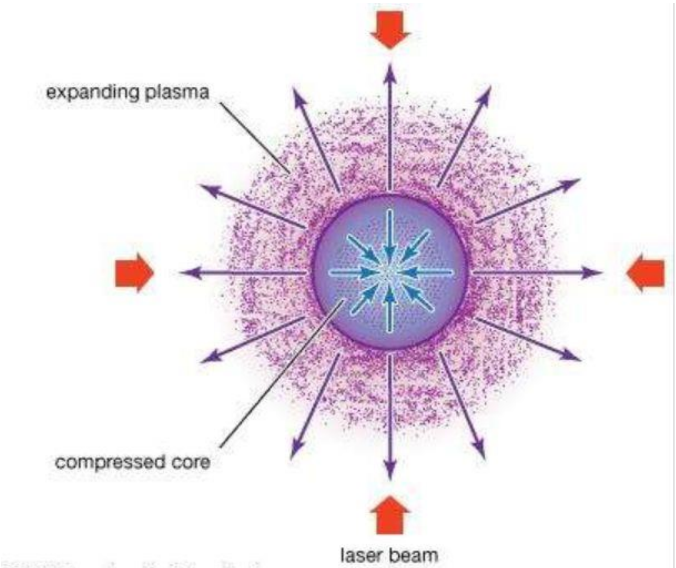

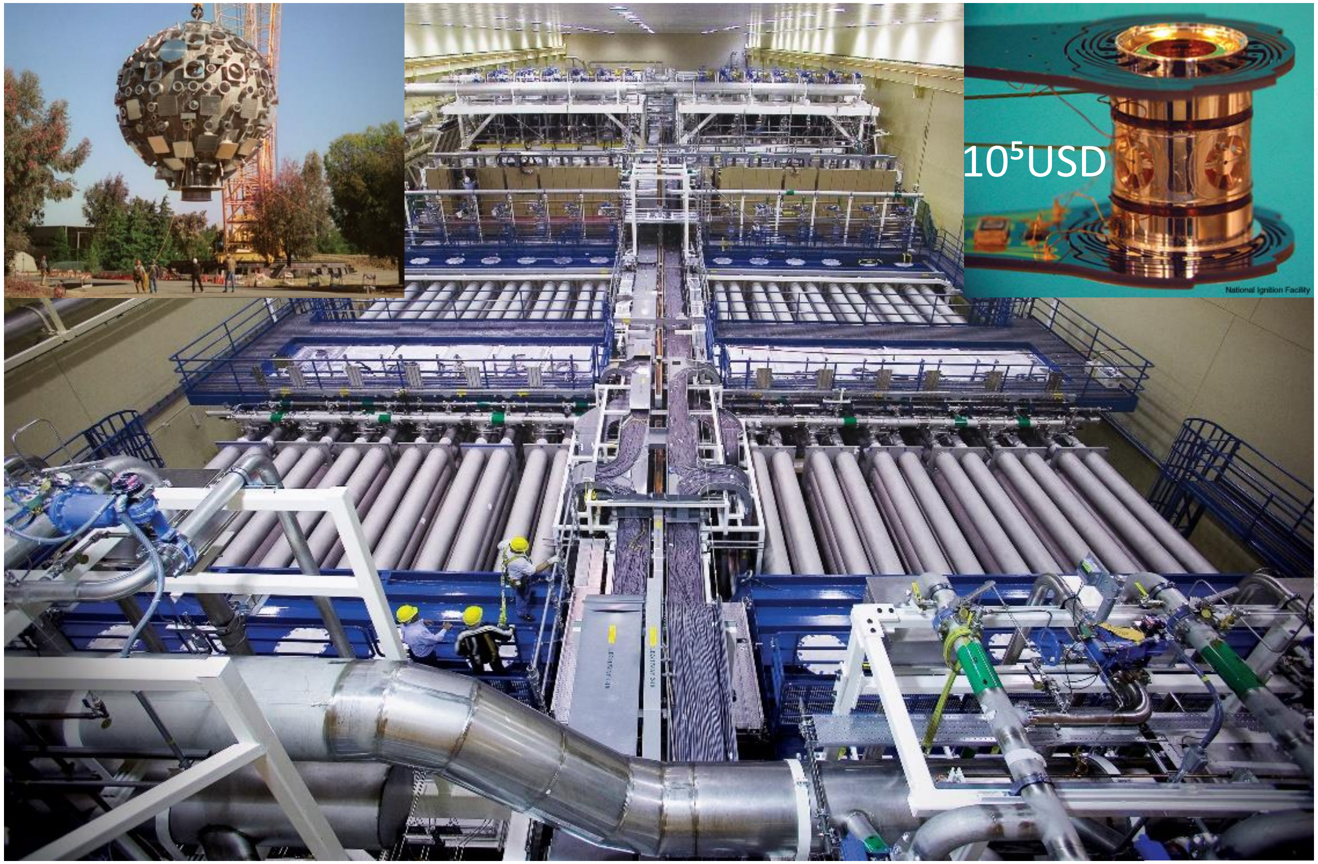


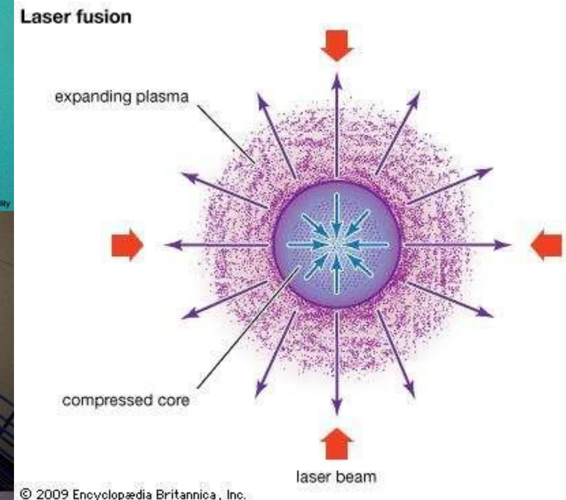


On the target:

**2MJ → 3MJ**

Long laser pulses (~50ns), 192 laser
Raileigh-Taylor instability
Complicated target construction
Enormous laser energy (400/2MJ)

## Problems of inertial fusion

- High requirements on irradiation symmetry
- Insufficient laser repetition rate
- Very precise injection system is needed
- The target position has to be tracked in order to ensure required irradiation precition

TO COMBINE 2 DIFFERENT (e.g. fusion and nano-) TECHNOLOGIES TO REACH FUSION AT THESE ULTRAHIGH EM FIELDS?

# No.2. application (LSPP)

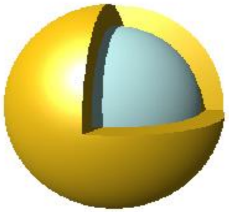

NANOSHELL
(nx10nm)

NANOROD (~85x25nm)

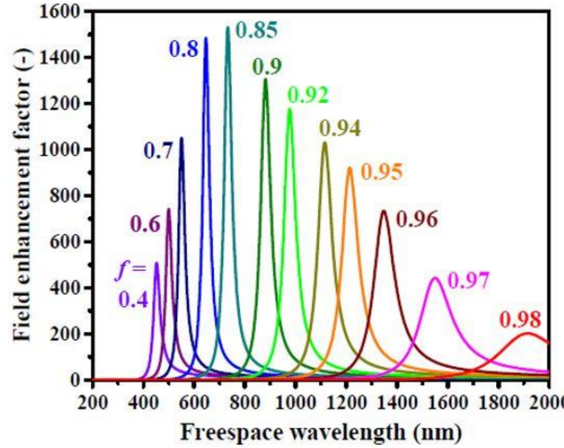


Λ = 800nm

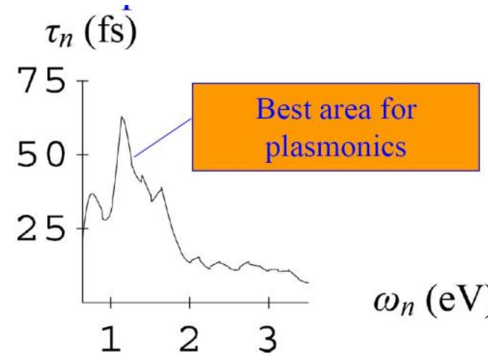


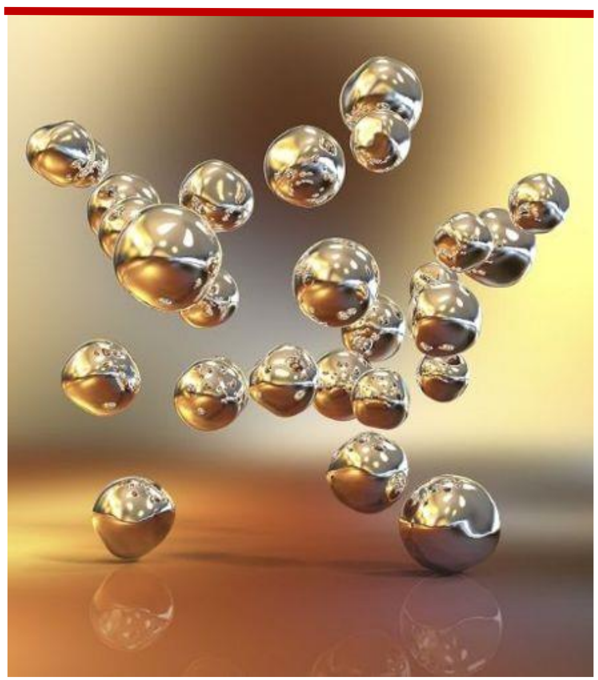

n.10μ

NANOPARTICLES IN
THE FUSION MATERIAL

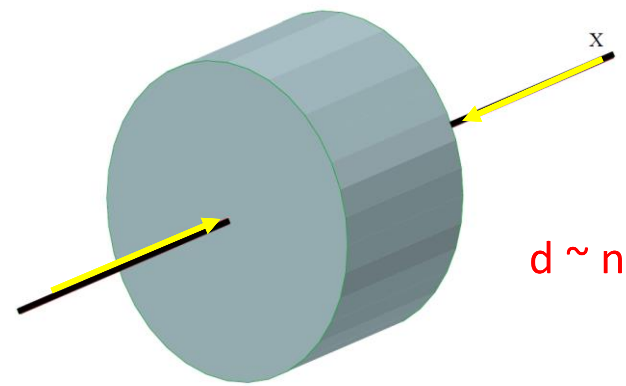


d ~ n.10μ

FEMTOSECOND LASER PULSES;
HIGH REPETITION FREQUENCY;
LIGHT SPEED: NO TIME FOR INSTABILITIES;
ONLY MAXIMUM TWO BEAMS;
(TIMELIKE VOLUME IGNITION)

AT PRESENT: RESULTS ONLY FROM ONE SIDED SHOTS.

Laser pulse length: 300 fs
Ti:Sa laser: Λ=800nm, ~1.55eV

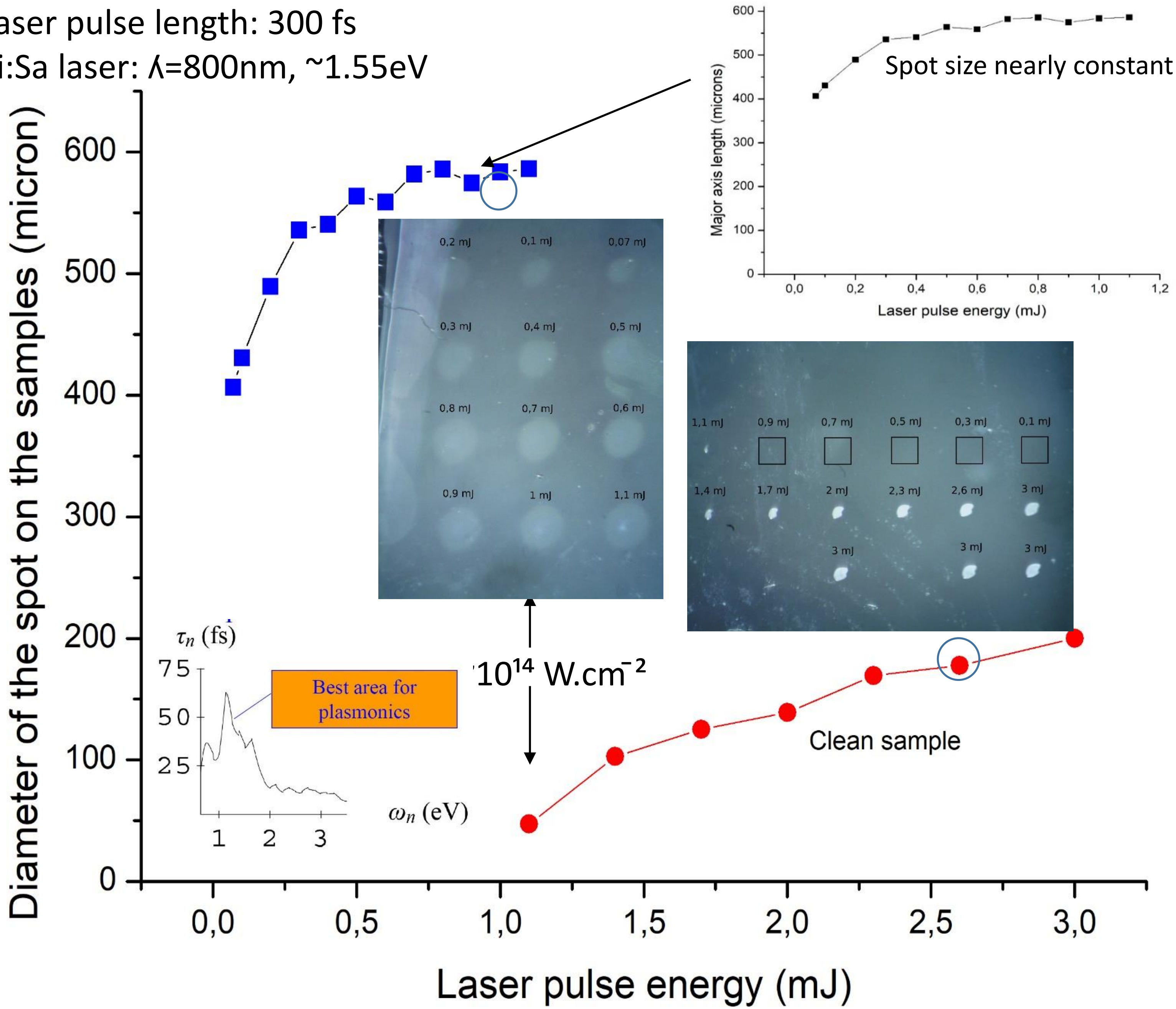


Giant plasmonic amplification; the laserlight reaches the nanoantennas;

# PLASMA MIRROR REFLECTIVITY

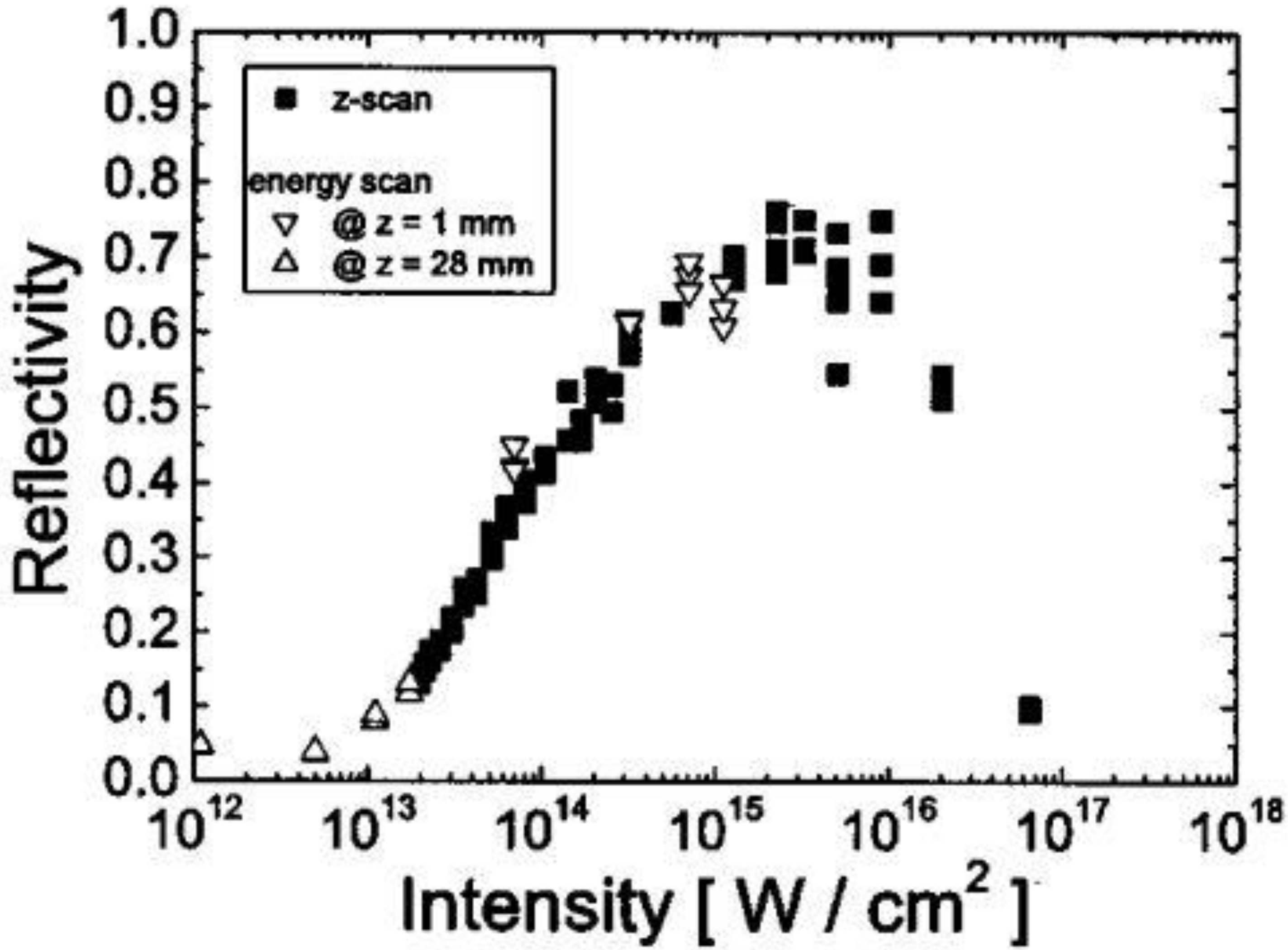


Ch.Ziener at al : J.Appl.Phys. 93,768 (2013)

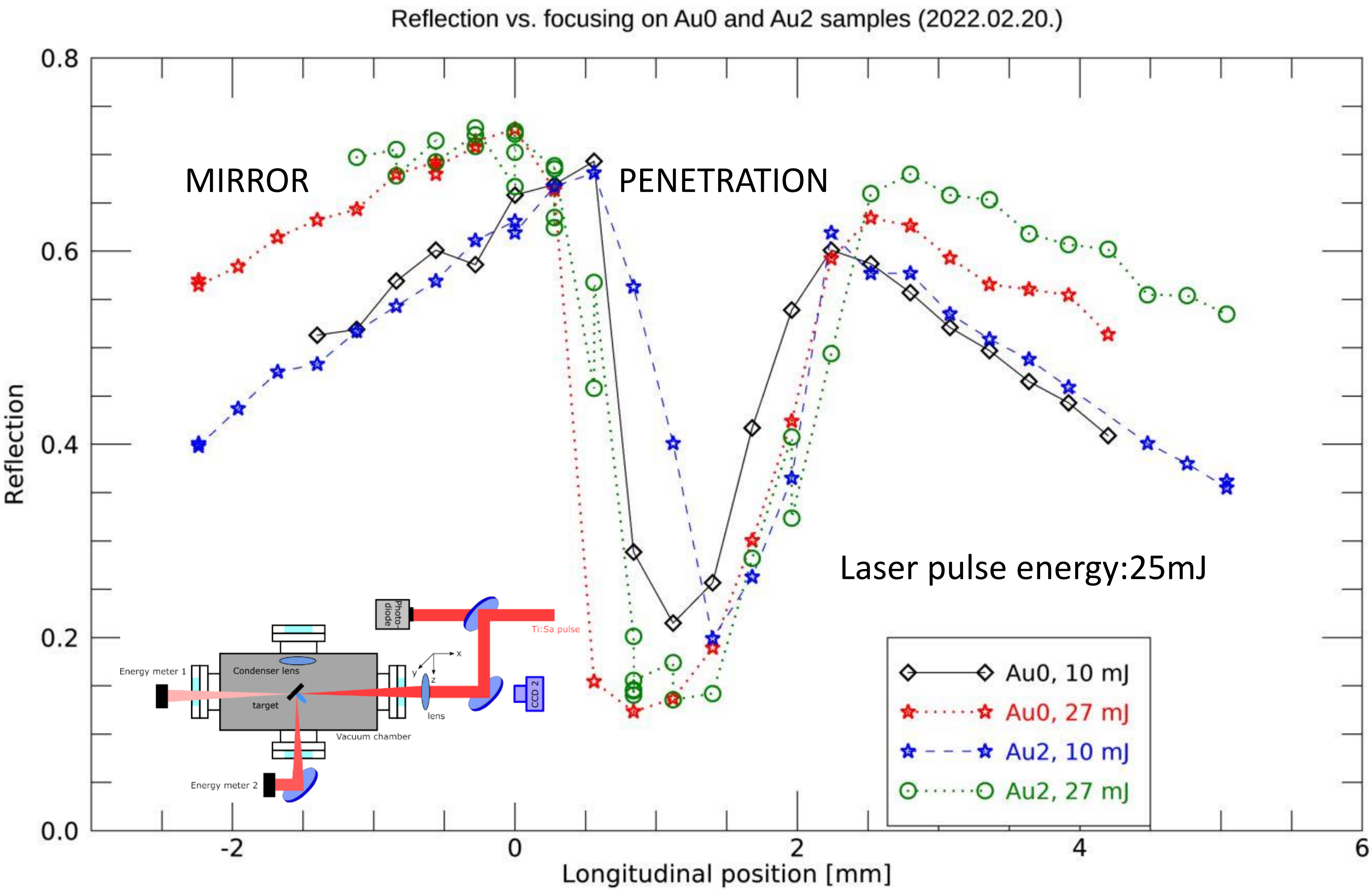


Sample: 160µm thick transparent polymer (UDMA).

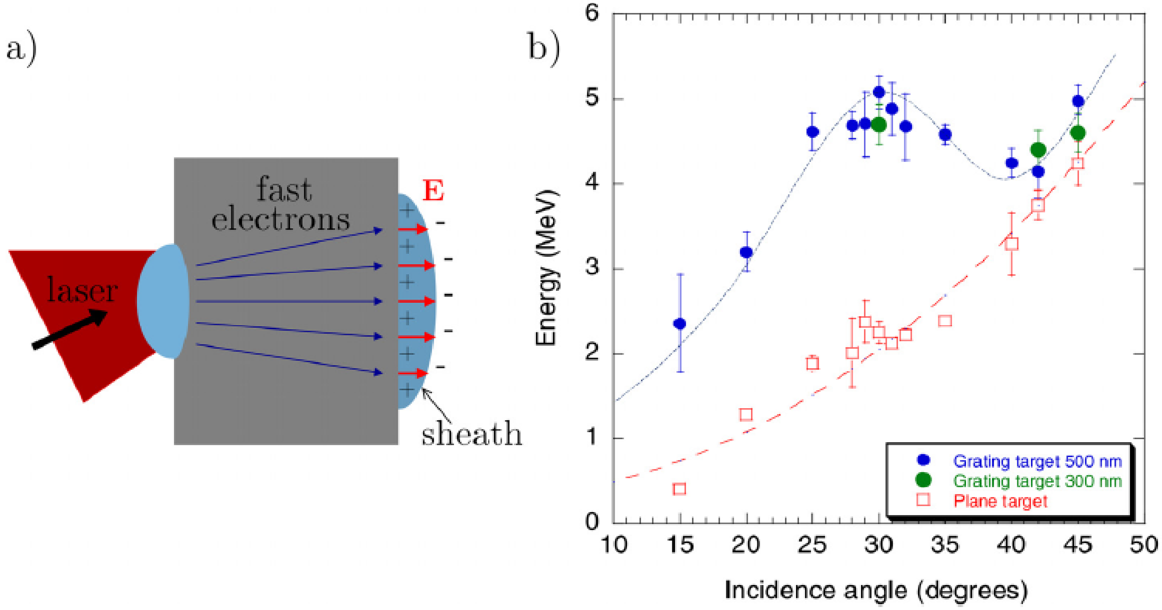


FIG. 5. Plasmon-enhanced TNSA of protons.[95] (a) Schematic of TNSA. The fast electrons produced by the interaction at the front side cross the target and produce a sheath at the rear side, where ions are accelerated. (b) Experimental data from the interactions of a high-contrast 25 fs, $2.5 \times 10^{19}$ W cm$^{-2}$ laser pulse with solid plastic targets. The cut-off energy of protons emitted from the rear measured as a function of the incidence angle from both flat and grating targets (for two different values of the grating depth). An up to 2.5-fold energy increase is observed for gratings, with a broad maximum around the resonant angle for SP excitation (30°). Data from Ref. 95.

Checcotti

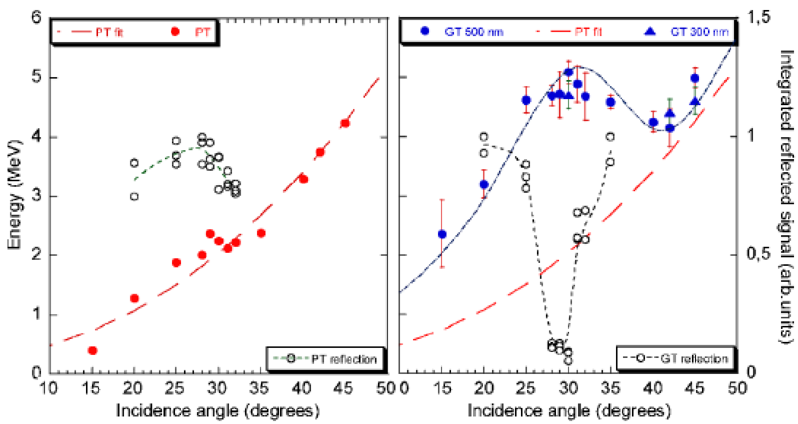


FIG. 3 (color online). Maximum proton energy (filled data points) and reflected light signal (empty data points) as a function of incidence angle $\alpha$. Left and right frames correspond to 20 $\mu$m thick plane targets and to 23 $\mu$m thick grating targets, respectively. Filled circles and triangles correspond to 0.5 and 0.3 $\mu$m deep gratings, respectively. The (red) dashed line is proportional to $\sin^2\alpha/\cos\alpha$. The other lines are guides for the eye.

## *Plasma absorption*

- A = 1-R

I < 3 x $10^{13}$ W cm$^{-2}$, A is almost polarization independent & obeys Fresnel laws, as IB is dominant

- at higher intensities, there is a clear polarization dependence of absorption

- the difference in absorption should account for extra absorption mechanisms, which are polarization dependent

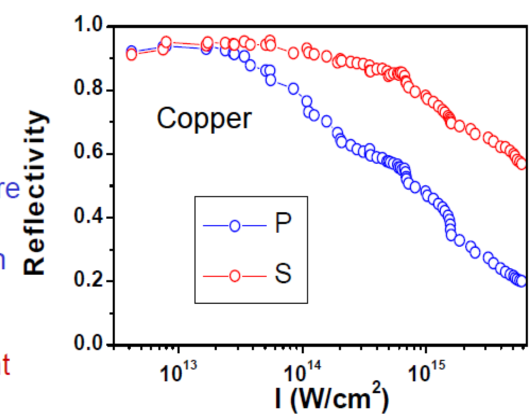


**R vs I at 45°**

*TIFR data*

# OUR PROPOSAL: COMBINE PLASMONICS WITH NUCLEAR FUSION TECHNOLOGY

SOME POTENTIALLY EXPLOITABLE HIGH FIELD PLASMONIC EFFECTS:

1.Go for localized surface plasmon polaritons (LSPP)

2.Lifetime of LSPP-s is in the few ten femtosecond range. We may get high intensity laser pulses in this time-domain and the plasma instabilities disappear.

3.High electron densities and EM fields can be obtained in small (nanosized) volumes on resonant plasmonic nanoparticles (hot spots).

4.The near field of plasmons screen the repulsive field of positively charged (e.g. protons) particles and so they may fuse more easily. So do the ponderomotive forces.

5.The large number of conduction electrons move in the plasmonic excitations in correlated way and their momentum may be in sum transfered in high exciting fields to positive particles, moving together with them, further increasing the probability of nuclear fusion.

6.With these short pulses we do not need many beams, like in the NIF, the target can be a thin film, illuminated only by 2 beams from opposite directions, and the same energy density may be achieved in the whole thicknes of the target sample, and this may

# ILLUSTRATION OF THE RESULT OF THE SCREENING EFFECT

HOT SPOTS

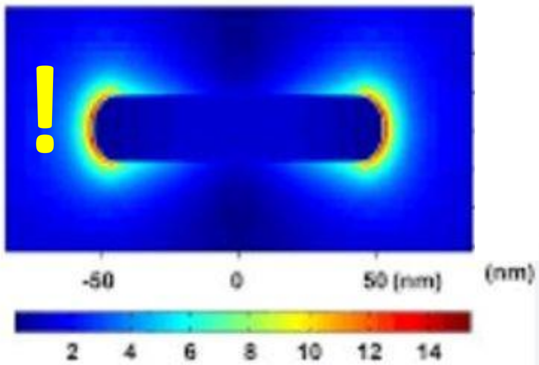

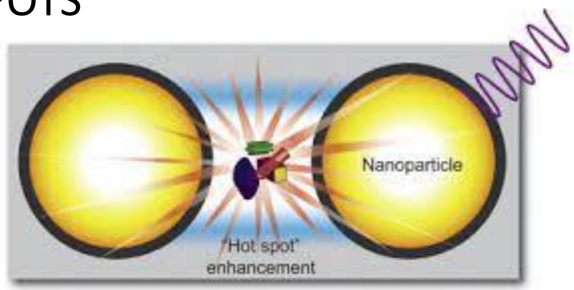


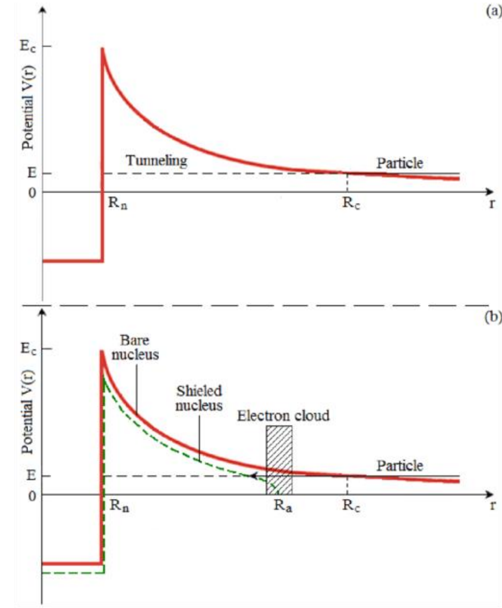


Ponderomotive screening

$F_p = (e^2/4m_e\omega^2).\mathrm{grad}\,(E^2)$

Illustration with the H+B ⟶ 3He reaction

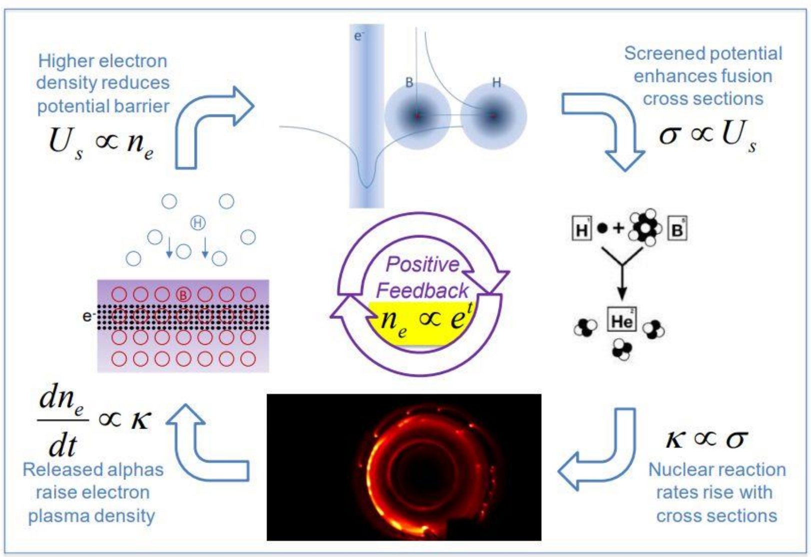


A.Y.Wong and C-C.Shinh:UCLA 2019

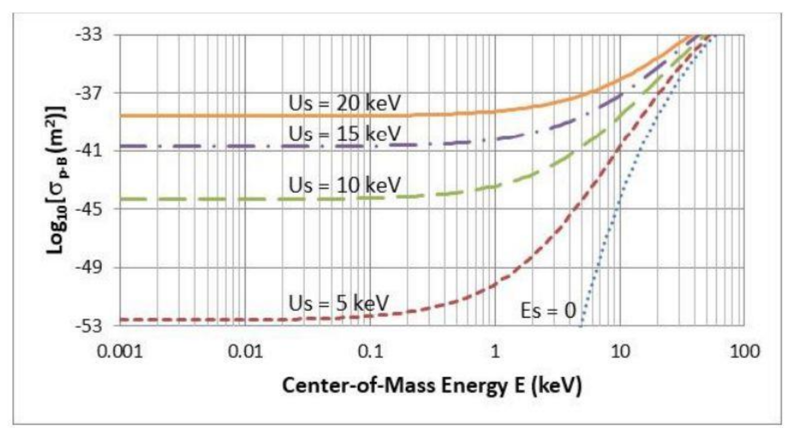


Figure 1: p-[11]B cross section as function of particle energy for the screening electron densities up to $E_s$ = 20keV. The cross section near $E$ = 10eV grows over 14 orders of magnitude (from $10^{-53}$ to $10^{-39}$m$^2$) over the range of 5 to 20keV.

# Demonstration of the correlated state

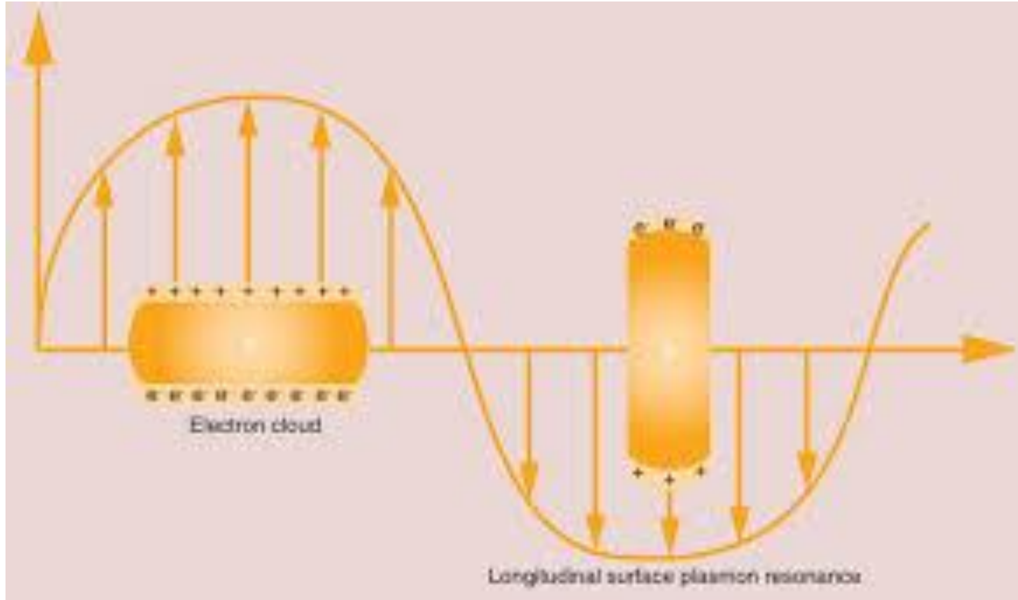


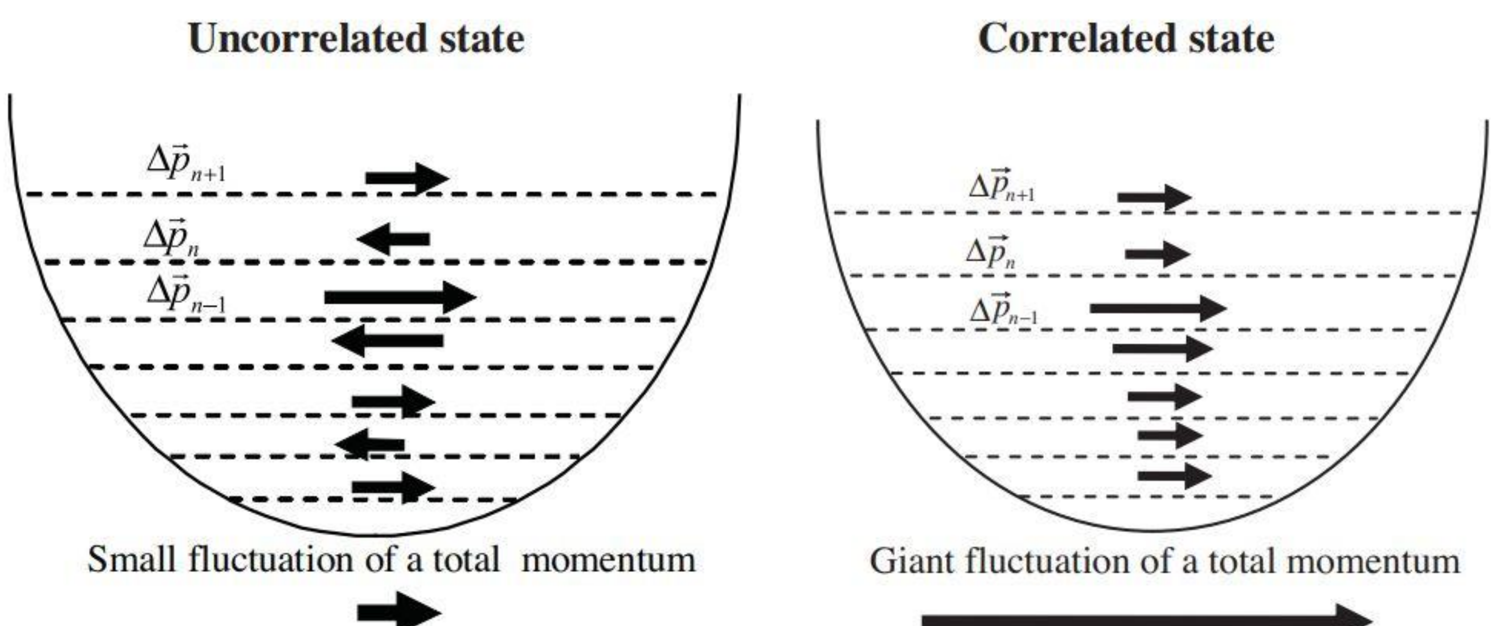

# SIMULATION OF PROTON AND ELECTRON ENERGIES AT A SINGLE NANOROD

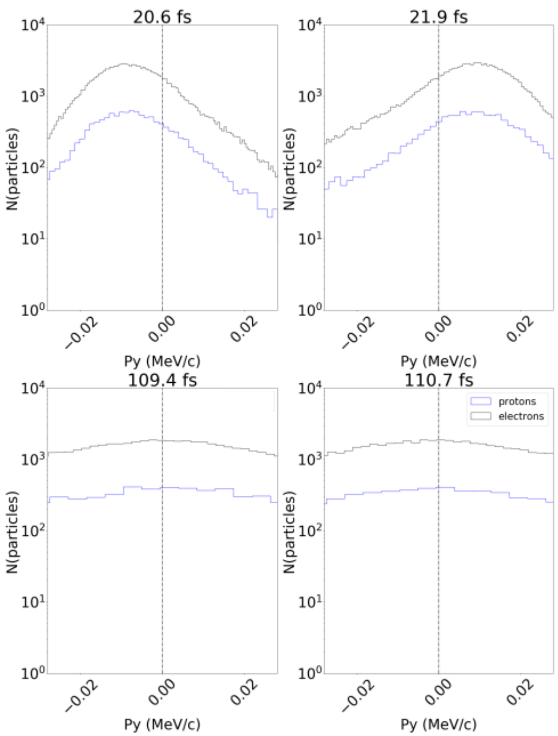


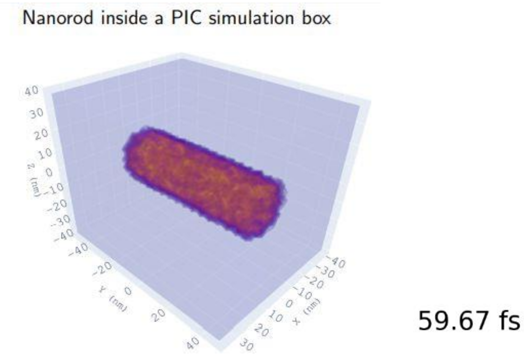


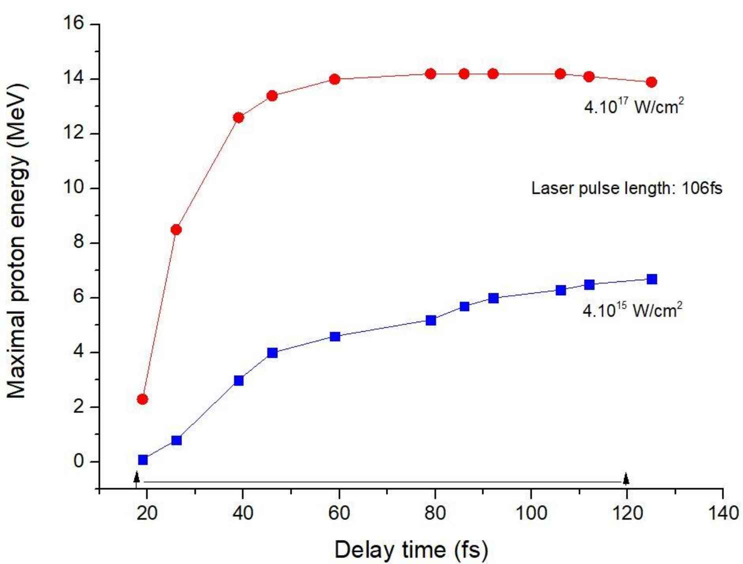


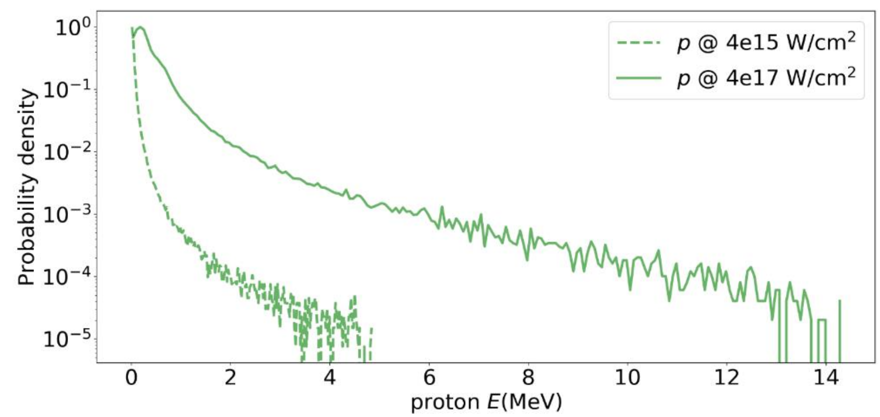


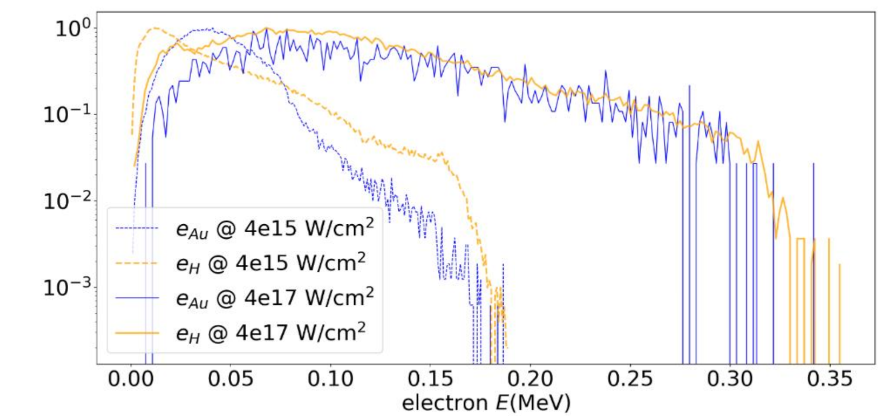

# With Au nanorods

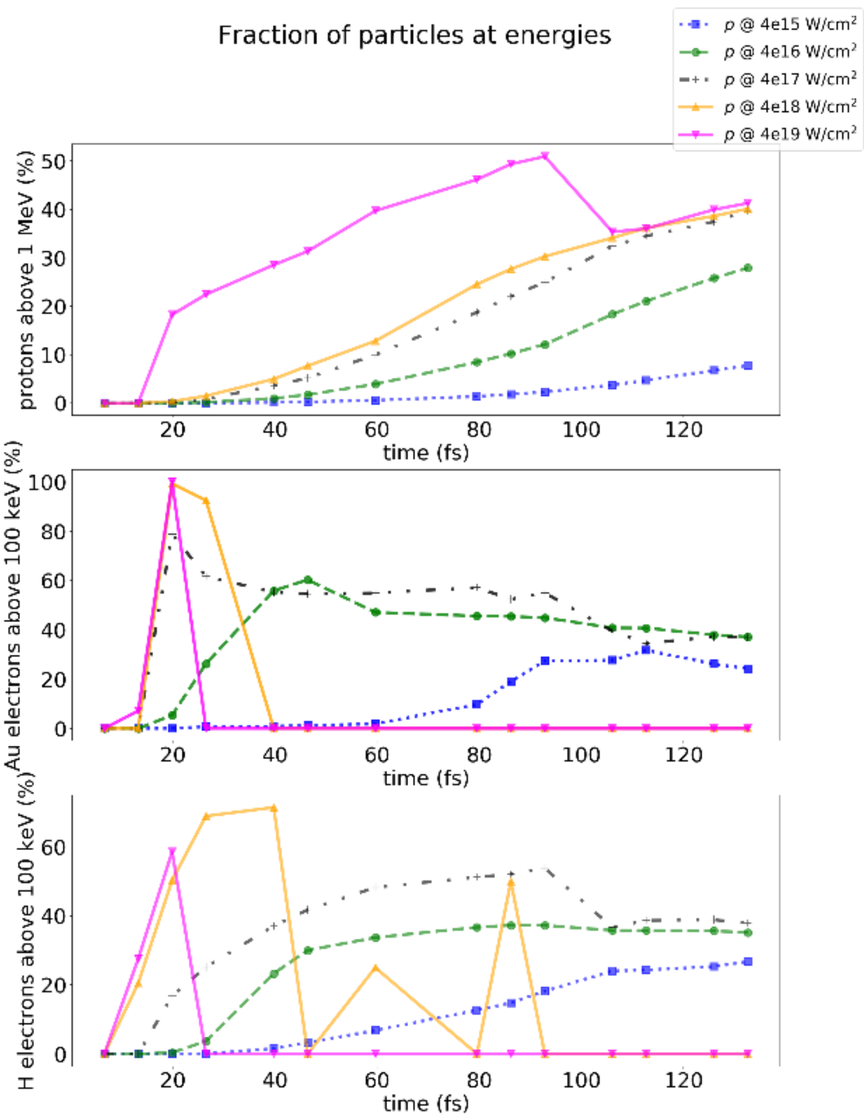


# Without Au nanorods

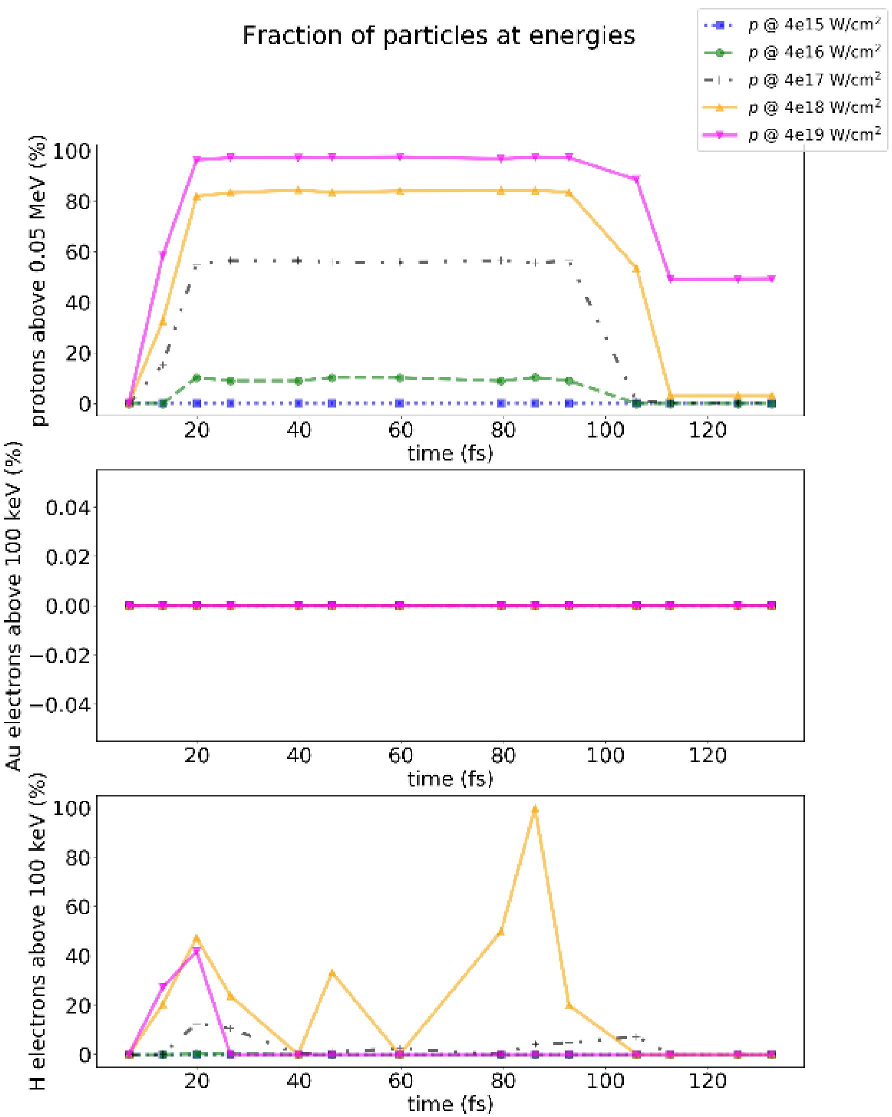

# Ti:Sa LASER PULSE SPECTRA AT DIFFERENT INTENSITIES

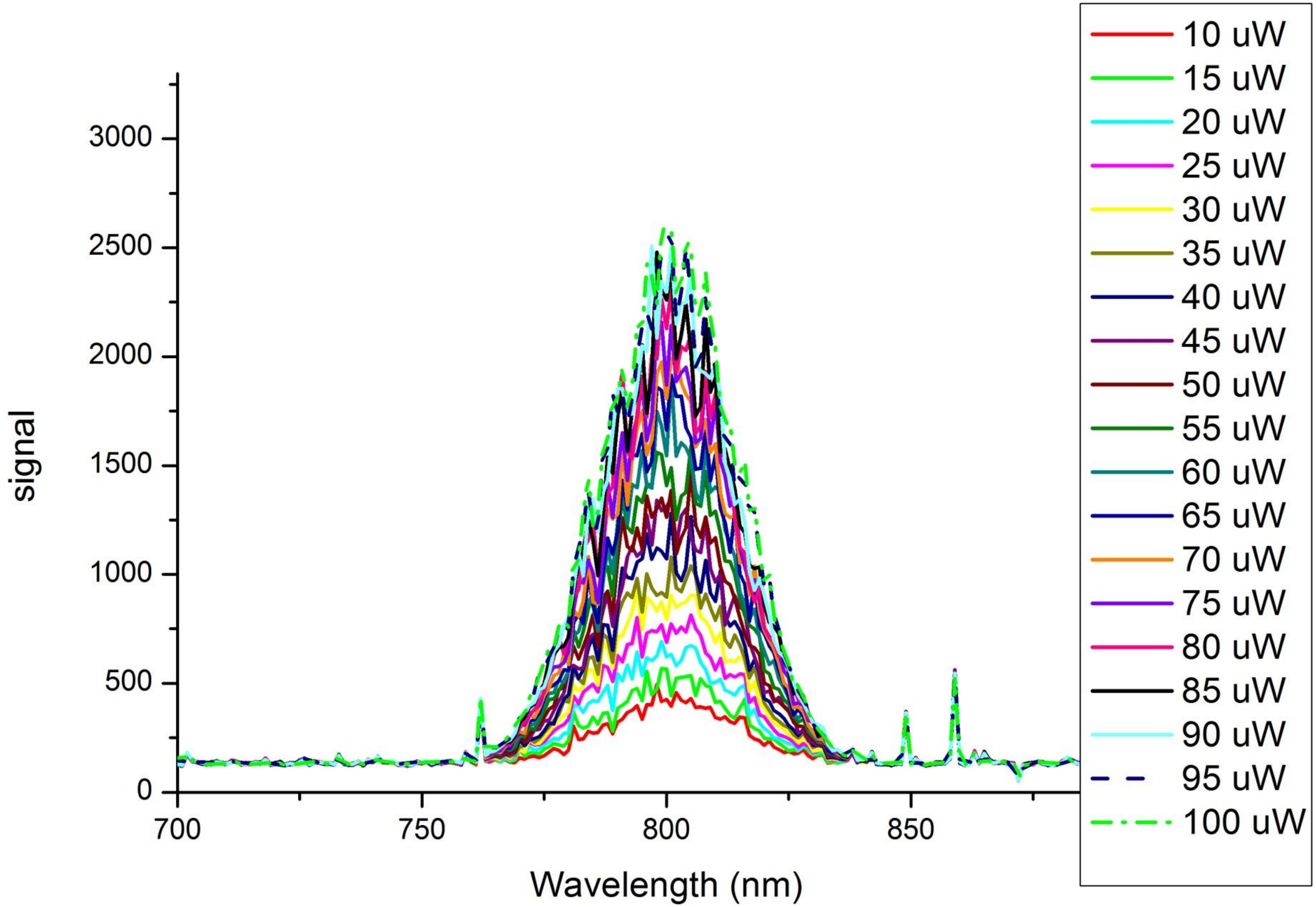

# The future:Two-sided irradiation

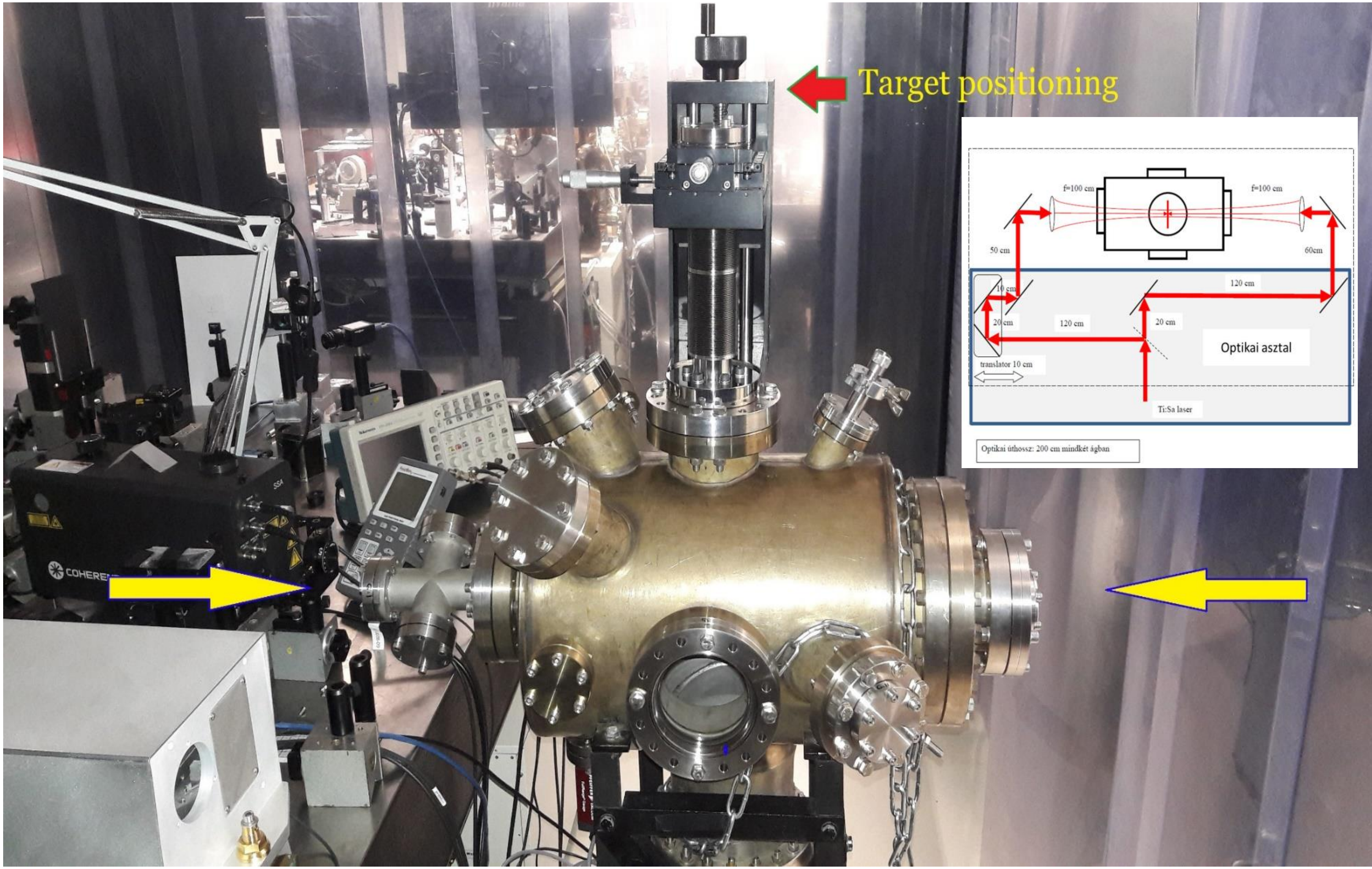

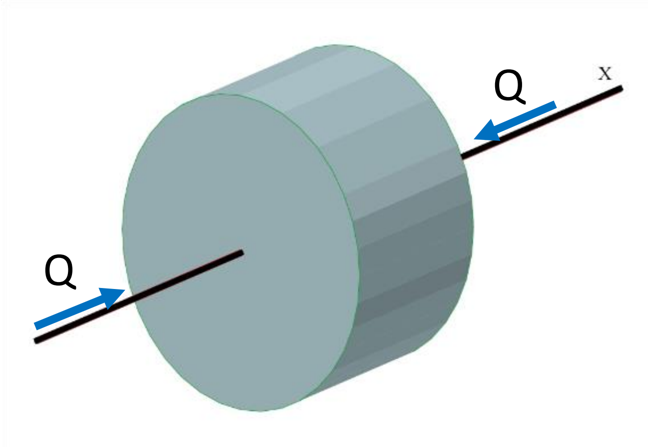


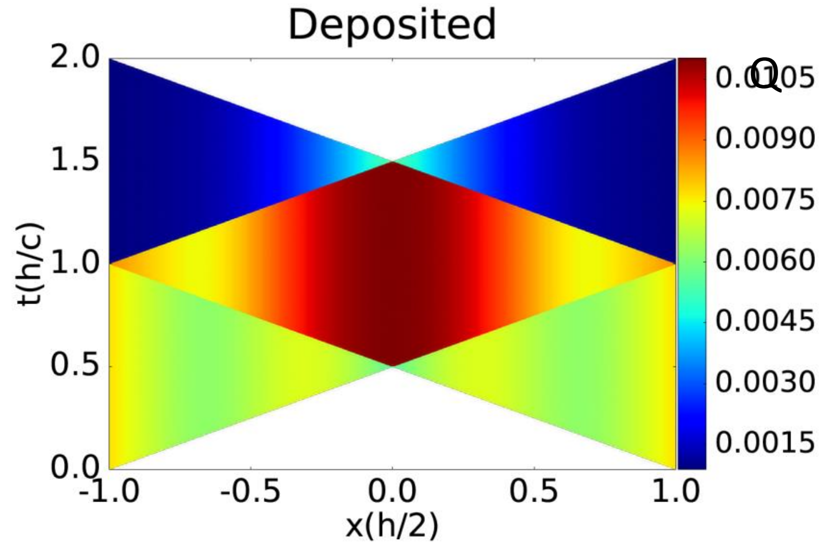


without nanoparticles

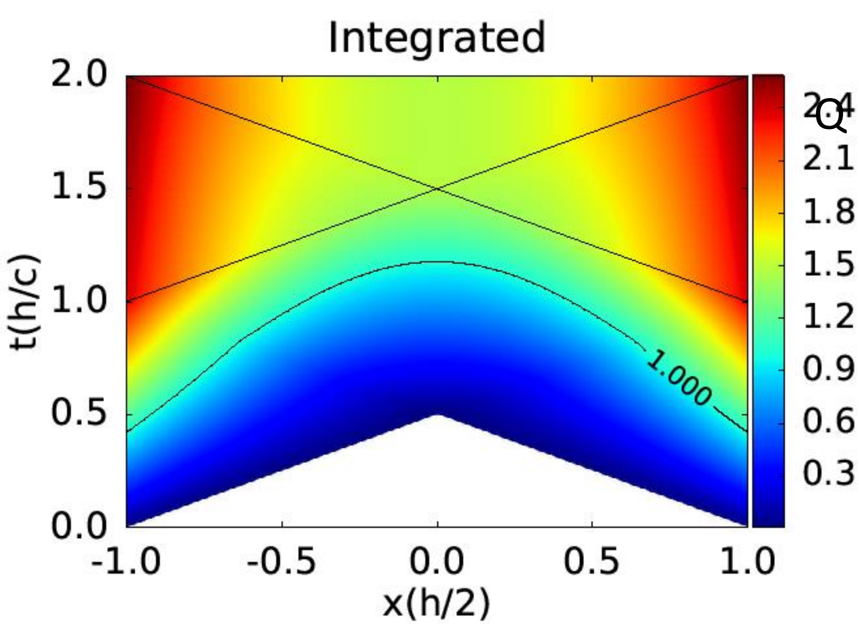


with nanoparticles

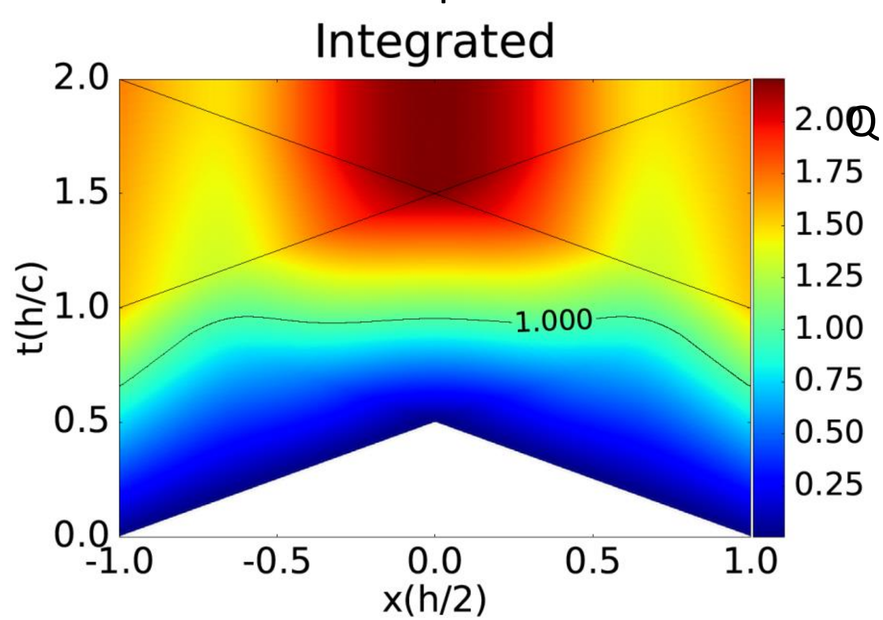


Some preliminary results with one side illumination

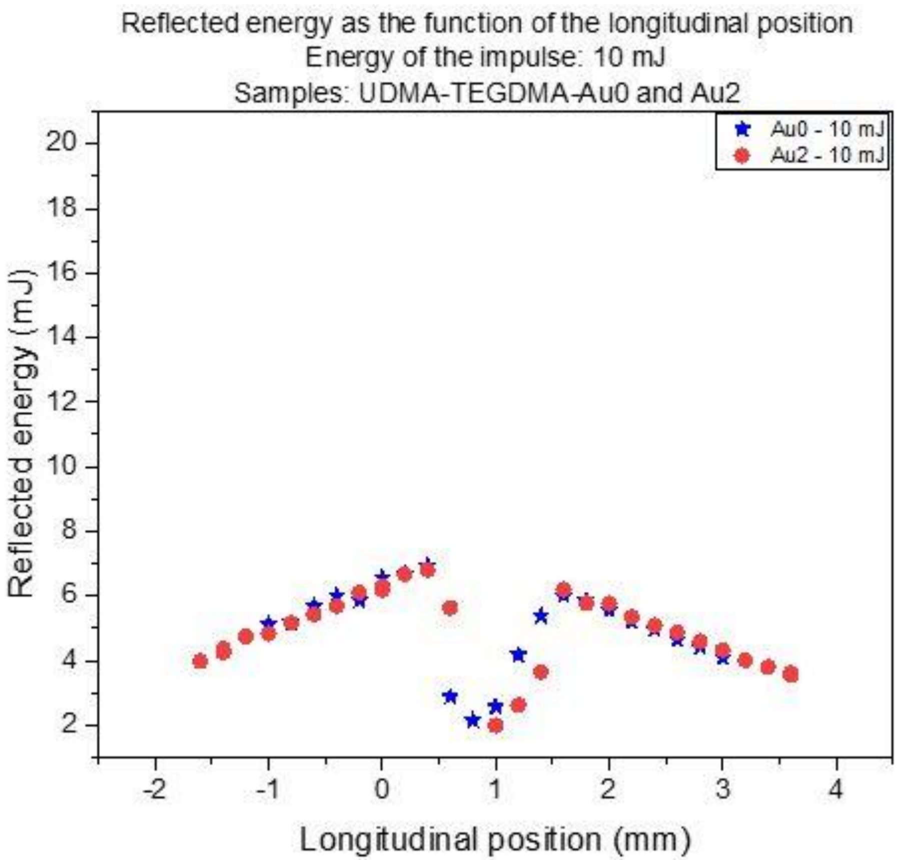
Reflected energy as the function of the longitudinal position
Energy of the impulse: 10 mJ
Samples: UDMA-TEGDMA-Au0 and Au2
Au0 - 10 mJ
Au2 - 10 mJ
Reflected energy (mJ)
Longitudinal position (mm)

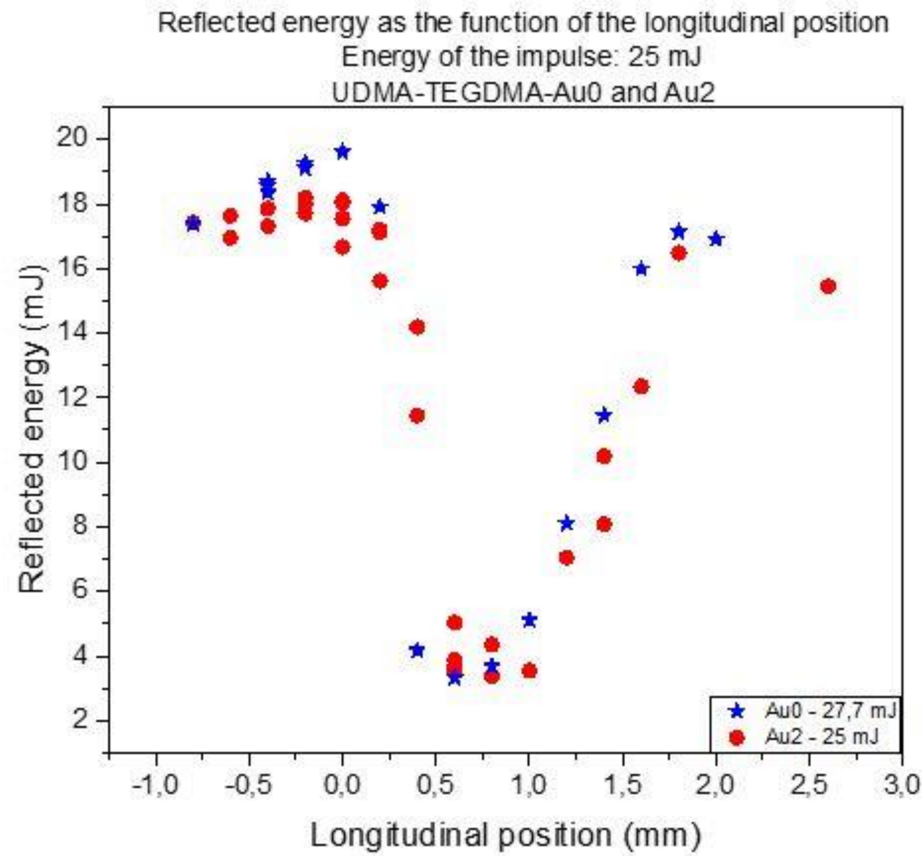
Reflected energy as the function of the longitudinal position
Energy of the impulse: 25 mJ
UDMA-TEGDMA-Au0 and Au2
Au0 - 27,7 mJ
Au2 - 25 mJ
Reflected energy (mJ)
Longitudinal position (mm)

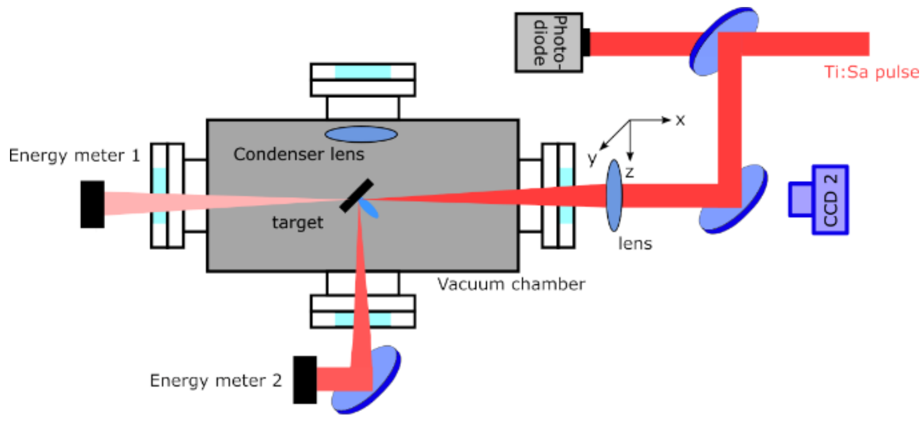
Photo-diode
Ti:Sa pulse
Energy meter 1
Condenser lens
target
lens
CCD 2
Vacuum chamber
Energy meter 2

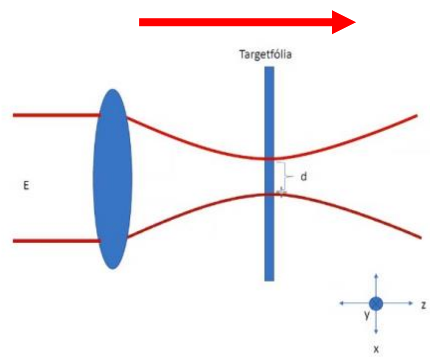
Targetfólia

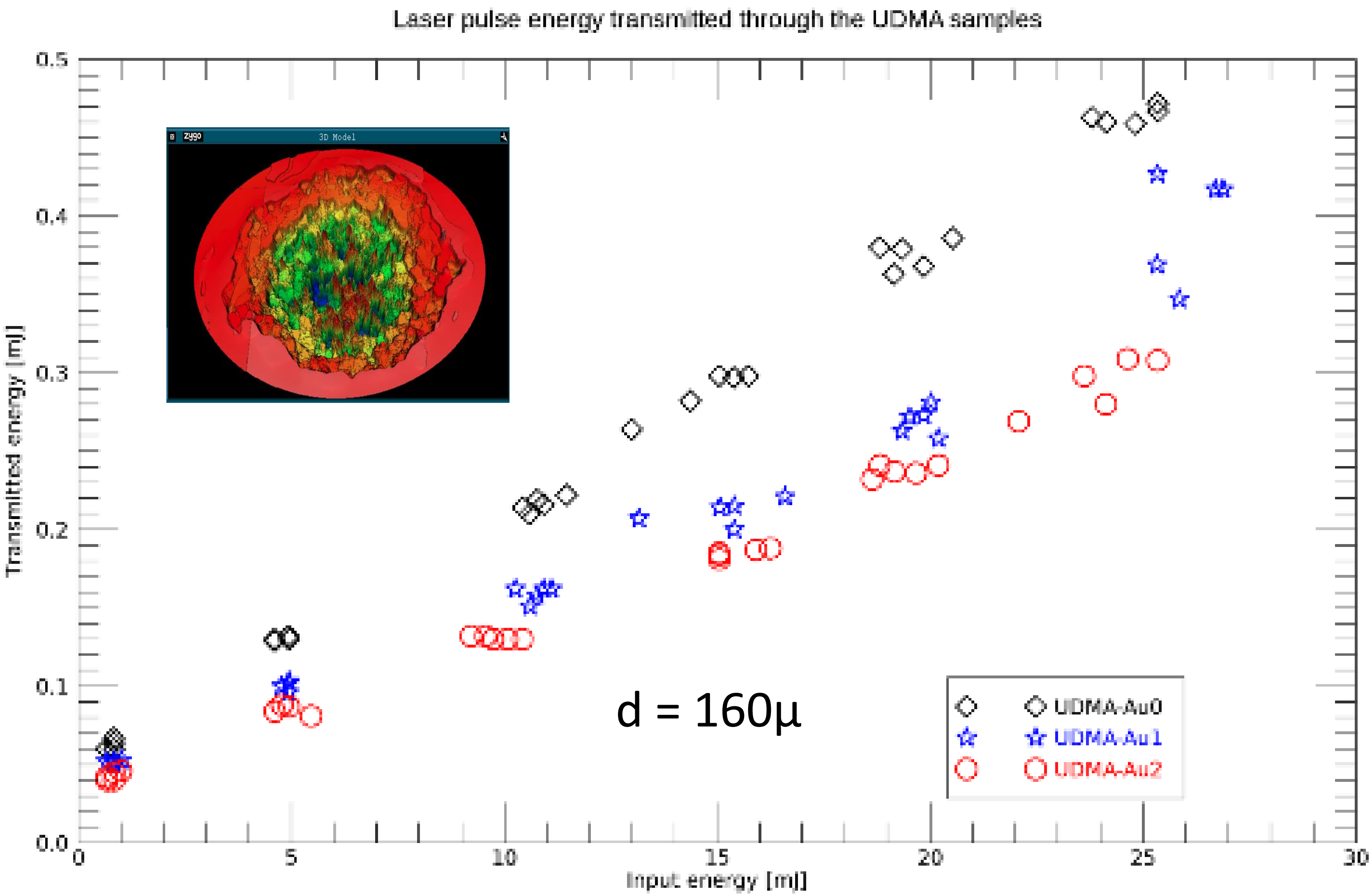

Laser pulse energy transmitted through the UDMA samples
Zygo
3D Model
Transmitted energy [mJ]
Input energy [mJ]
0.0
0.1
0.2
0.3
0.4
0.5
0
5
10
15
20
25
30
d = 160μ
UDMA-Au0
UDMA-Au1
UDMA-Au2

# 1. DIAGNOSIS

SEM IMAGE OF UDMA WITH AU NANORODS SEM IMAGE OF UDMA WITHOUT AU NANORODS
And Zygo images of the craters

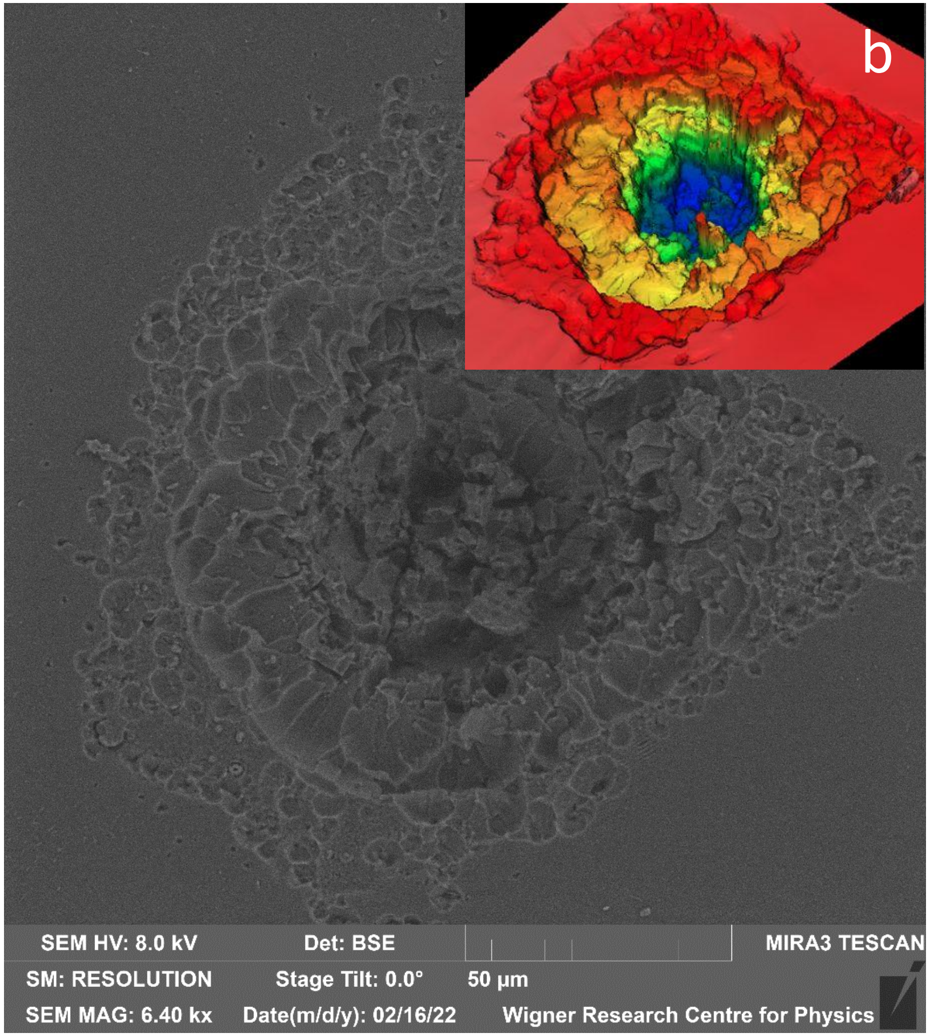


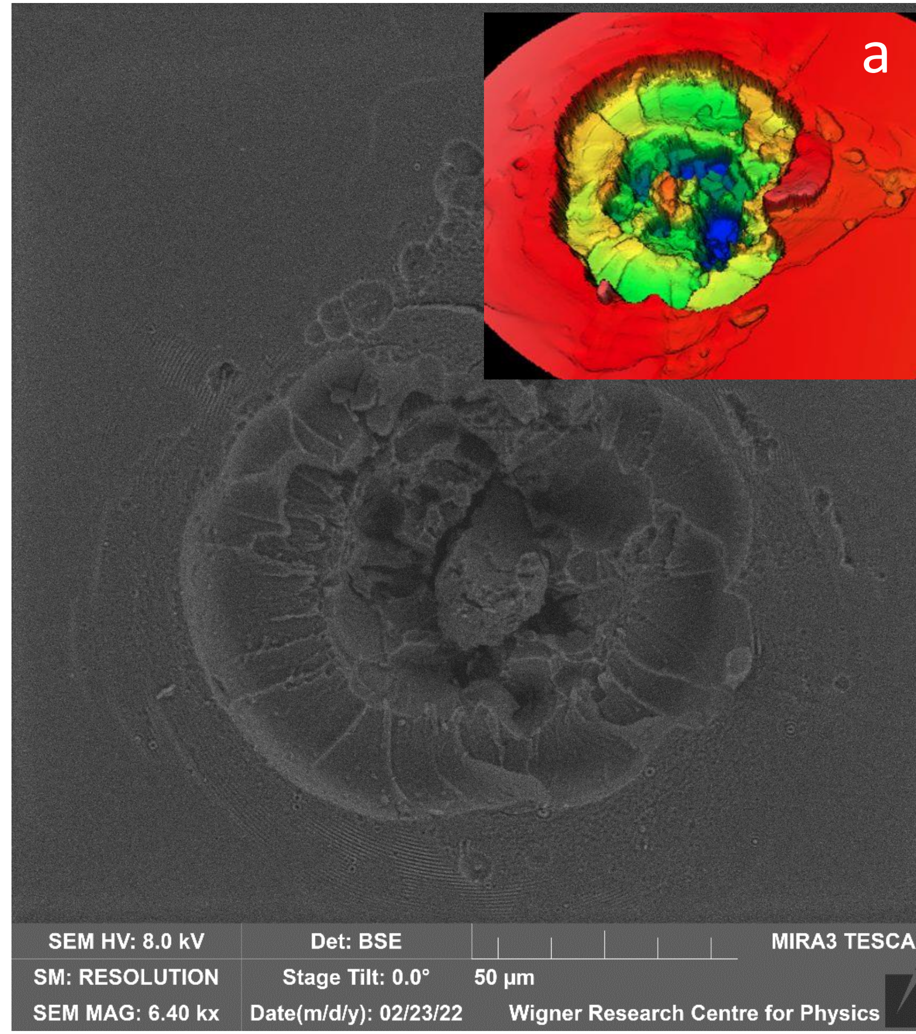


Images at 17.5mJ laser energy, $1,16.10^{17}$ W/cm$^2$ laser intensity.The volume of the crater of the sample with nanorods (b) is 1.98 times that of the sample without rods (a).

# DIAGNOZIS (crater volume)

Volume: $V_0$

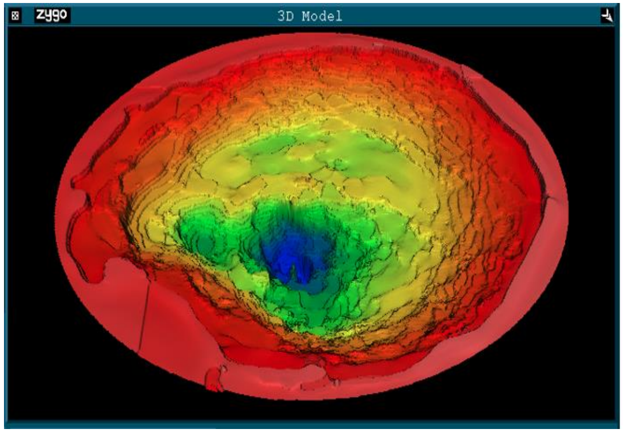


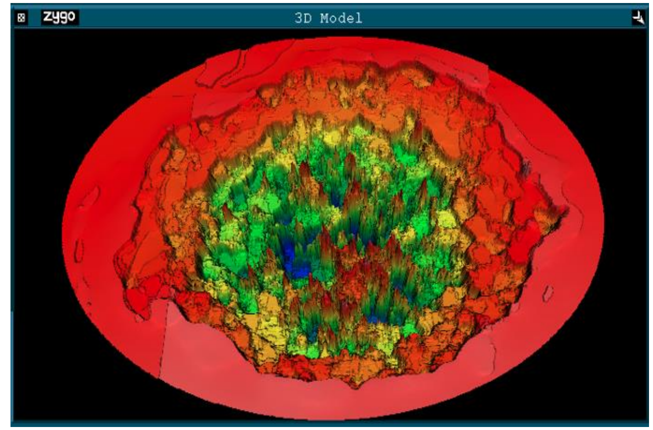


Volume max. $3.5V_0$

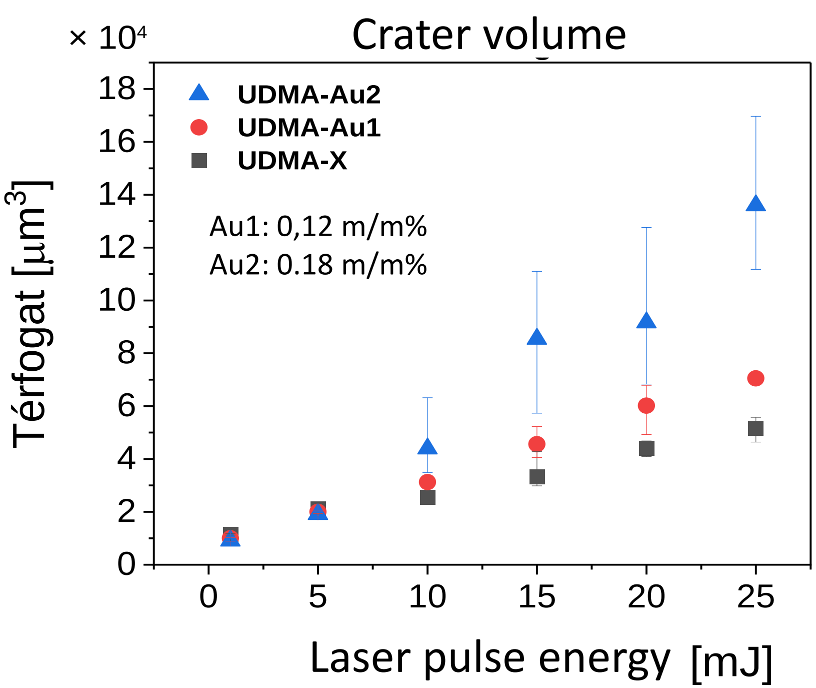


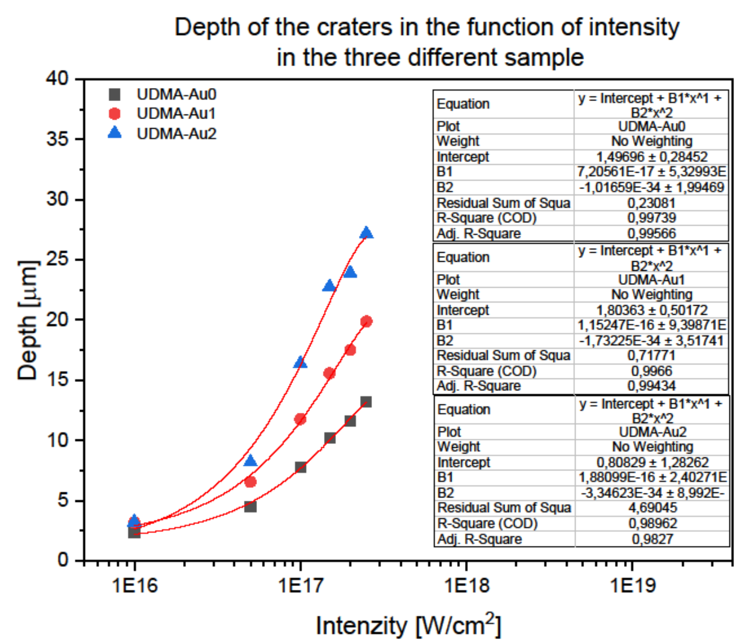


| | |
|---|---|
| Equation | y = Intercept + B1*x^1 + B2*x^2 |
| Plot | UDMA-Au0 |
| Weight | No Weighting |
| Intercept | 1,49696 ± 0,28452 |
| B1 | 7,20561E-17 ± 5,32993E |
| B2 | -1,01659E-34 ± 1,99469 |
| Residual Sum of Squa | 0,23081 |
| R-Square (COD) | 0,99739 |
| Adj. R-Square | 0,99566 |
| Equation | y = Intercept + B1*x^1 + B2*x^2 |
| Plot | UDMA-Au1 |
| Weight | No Weighting |
| Intercept | 1,80363 ± 0,50172 |
| B1 | 1,15247E-16 ± 9,39871E |
| B2 | -1,73225E-34 ± 3,51741 |
| Residual Sum of Squa | 0,71771 |
| R-Square (COD) | 0,9966 |
| Adj. R-Square | 0,99434 |
| Equation | y = Intercept + B1*x^1 + B2*x^2 |
| Plot | UDMA-Au2 |
| Weight | No Weighting |
| Intercept | 0,80829 ± 1,28262 |
| B1 | 1,88099E-16 ± 2,40271E |
| B2 | -3,34623E-34 ± 8,992E- |
| Residual Sum of Squa | 4,69045 |
| R-Square (COD) | 0,98962 |
| Adj. R-Square | 0,9827 |

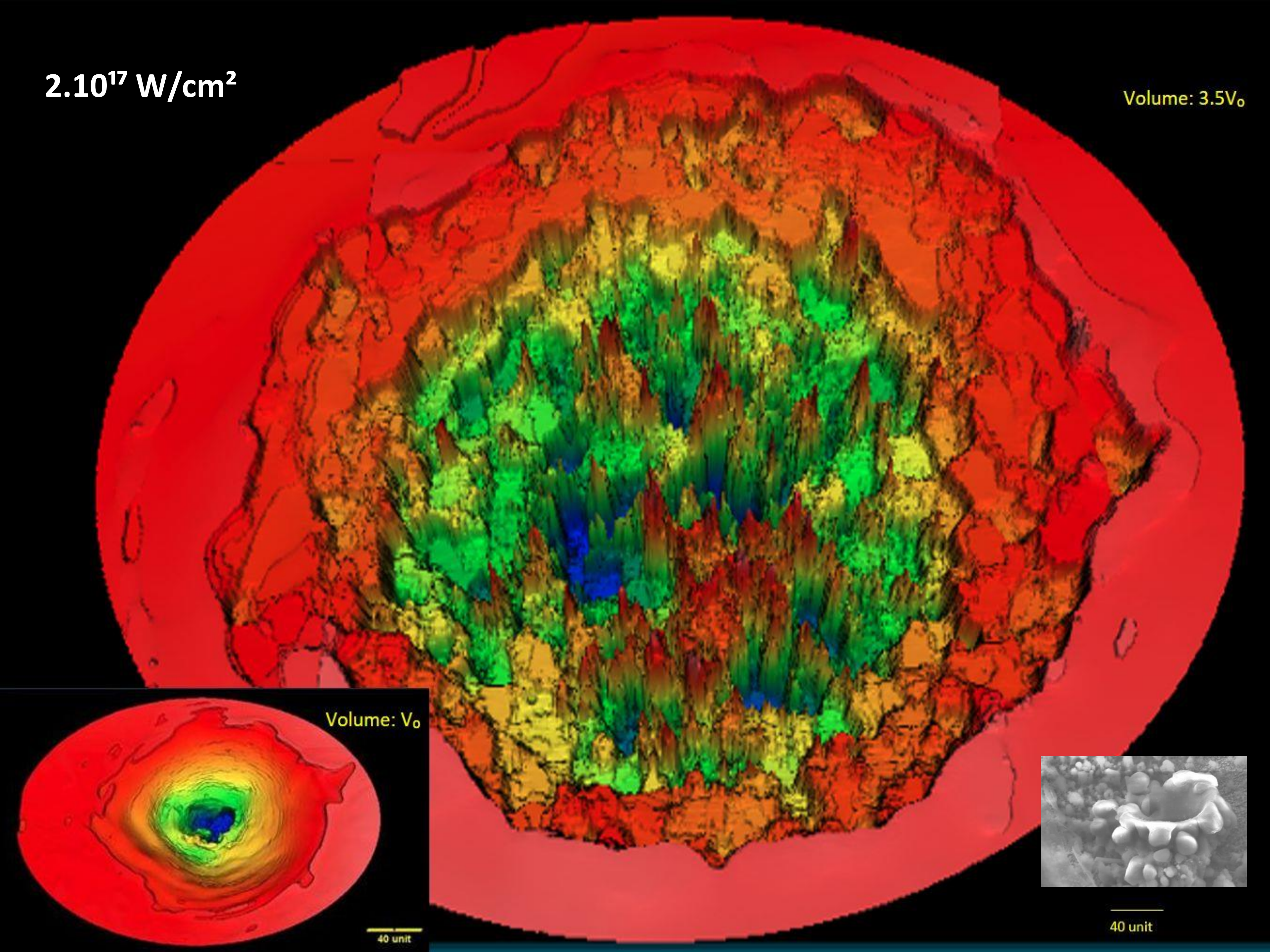
2.10$^{17}$ W/cm$^2$
Volume: 3.5V$_0$
Volume: V$_0$
40 unit
40 unit

# CRATER VOLUMES

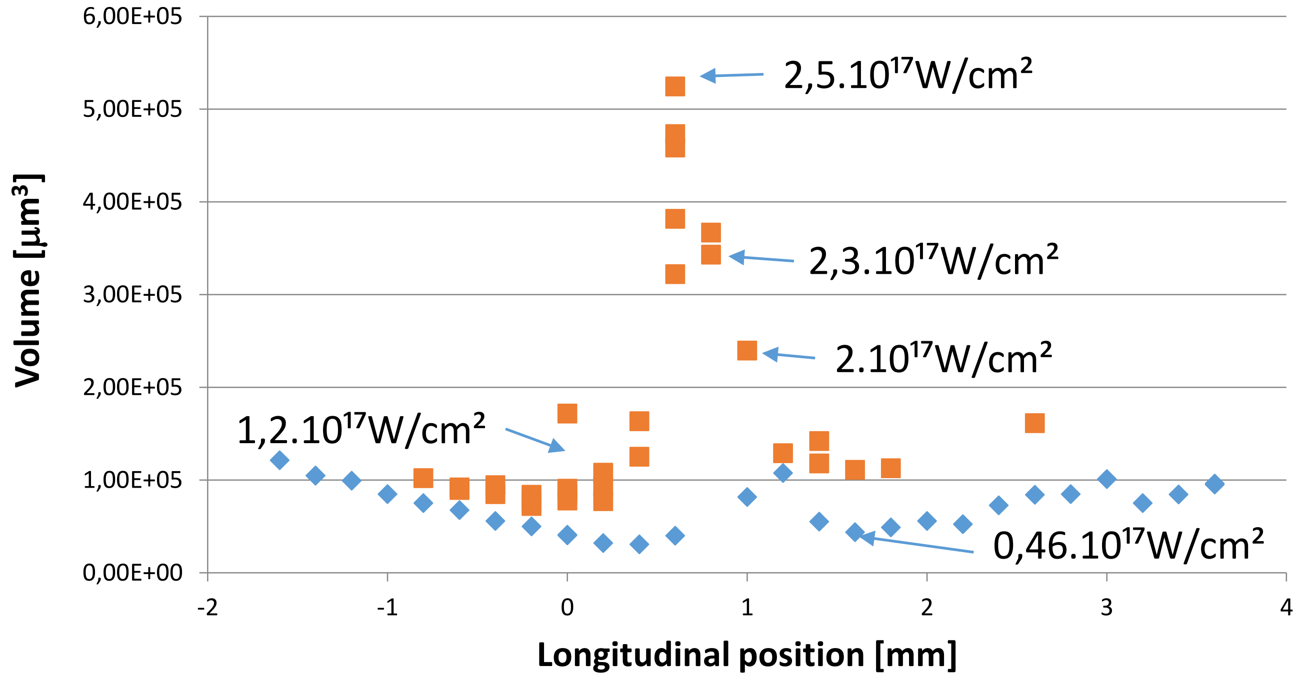


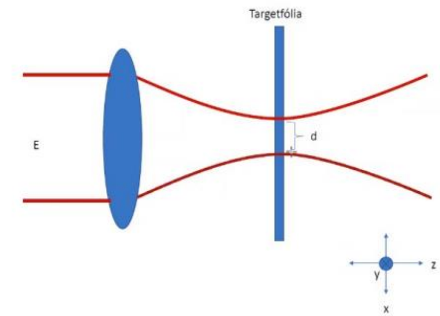


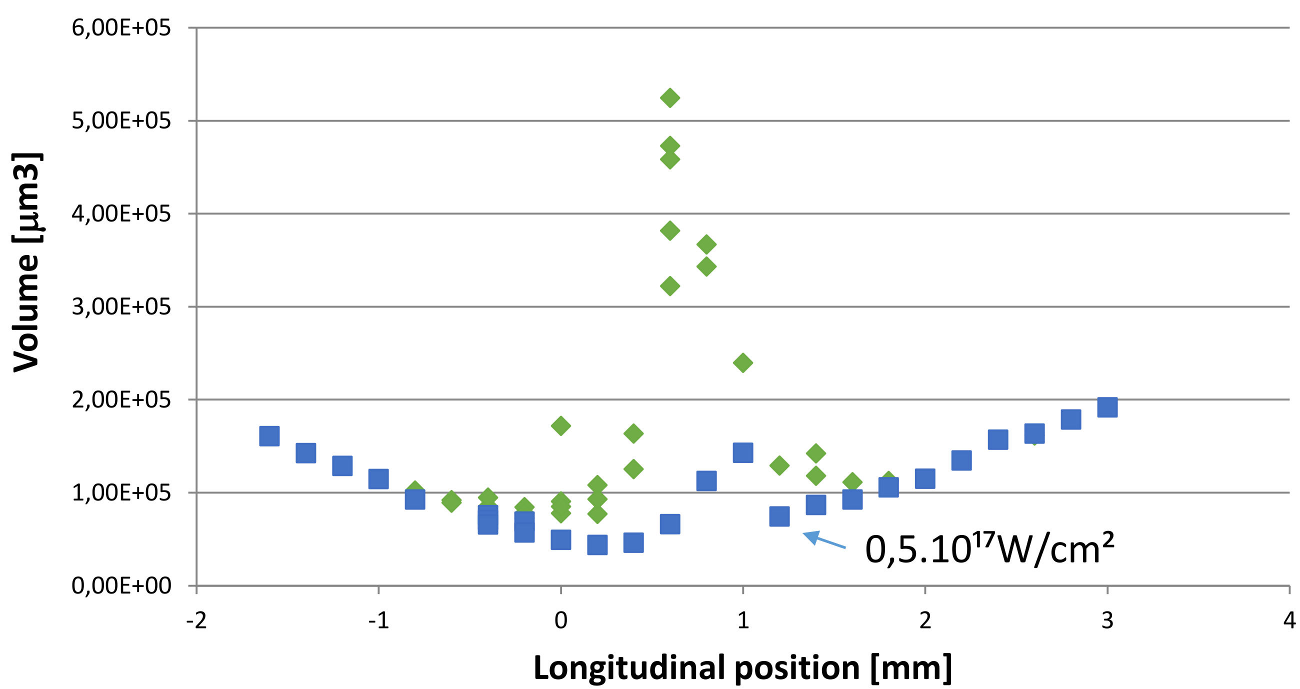


**HIGH FIELD PLASMONICS WORKS!**

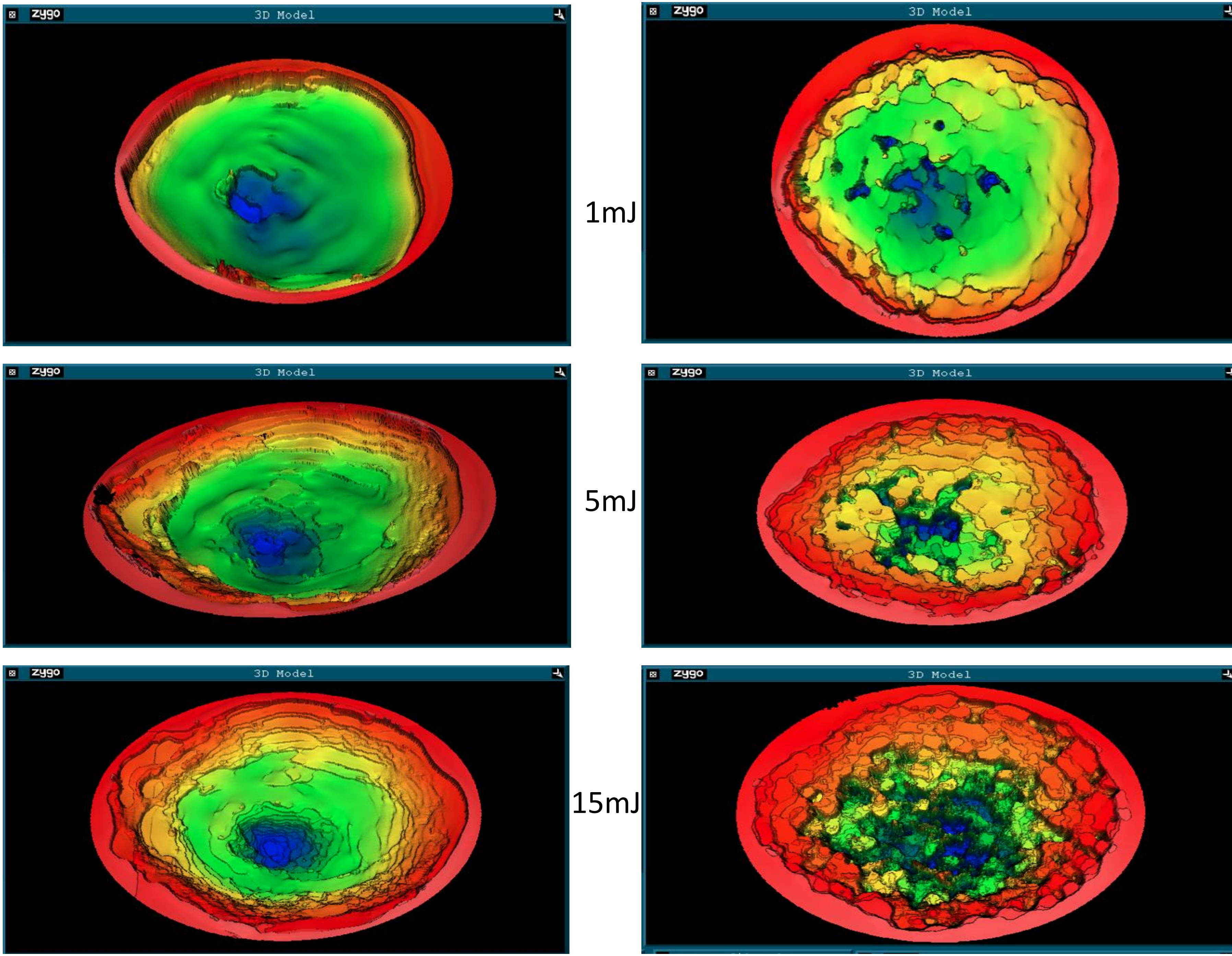
zygo
3D Model
1mJ
5mJ
15mJ

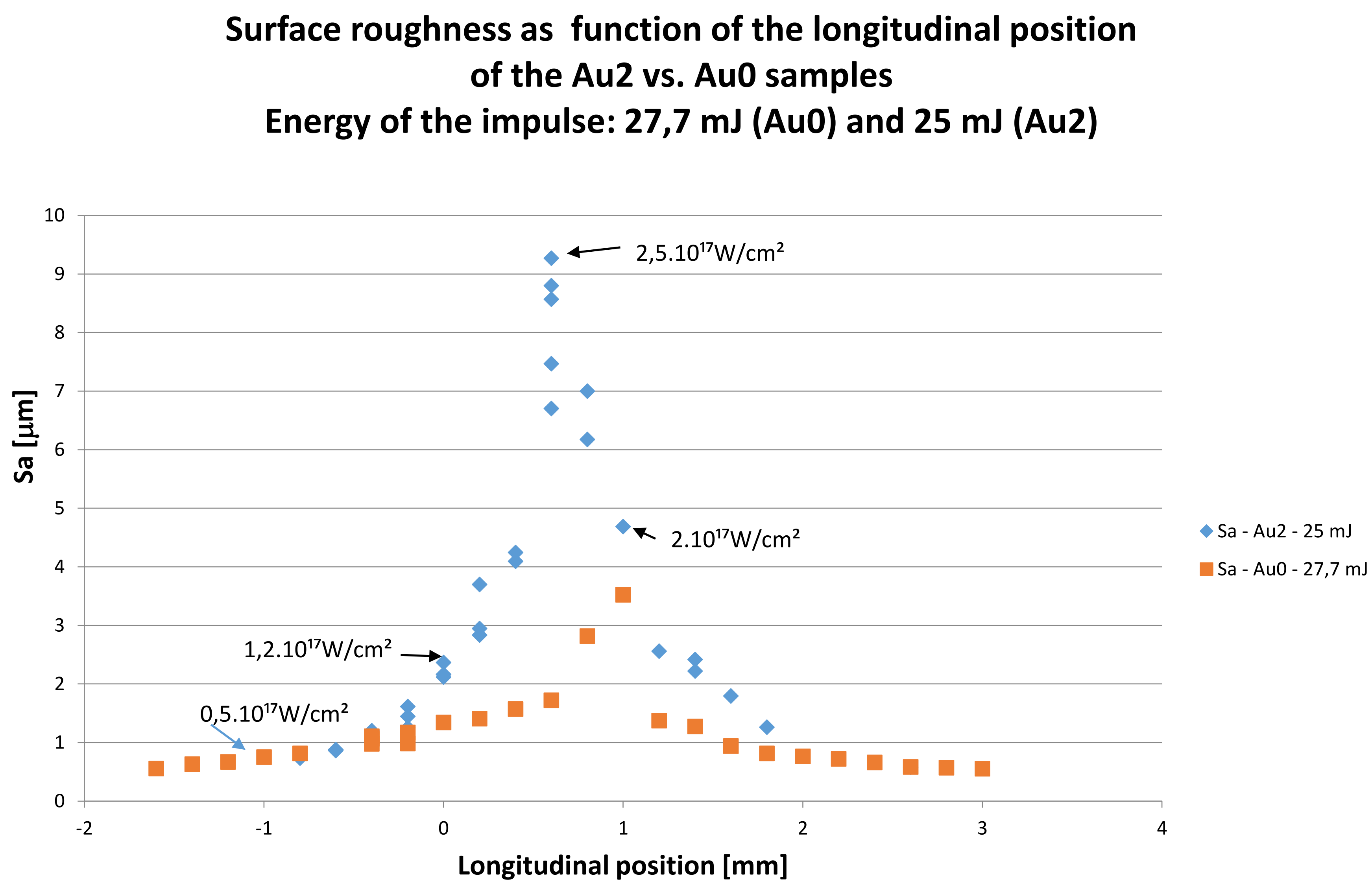

Surface roughness as function of the longitudinal position
of the Au2 vs. Au0 samples
Energy of the impulse: 27,7 mJ (Au0) and 25 mJ (Au2)
2,5.10¹⁷W/cm²
2.10¹⁷W/cm²
1,2.10¹⁷W/cm²
0,5.10¹⁷W/cm²
Sa [µm]
Longitudinal position [mm]
Sa - Au2 - 25 mJ
Sa - Au0 - 27,7 mJ

# CRATER VOLUMES

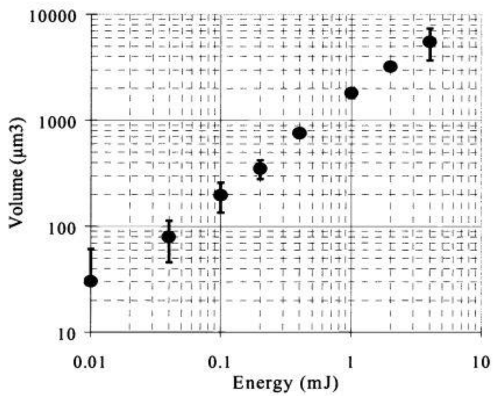


Fig. 4. Dependence of crater volume on laser energy for copper. (532 nm, 6 ns)

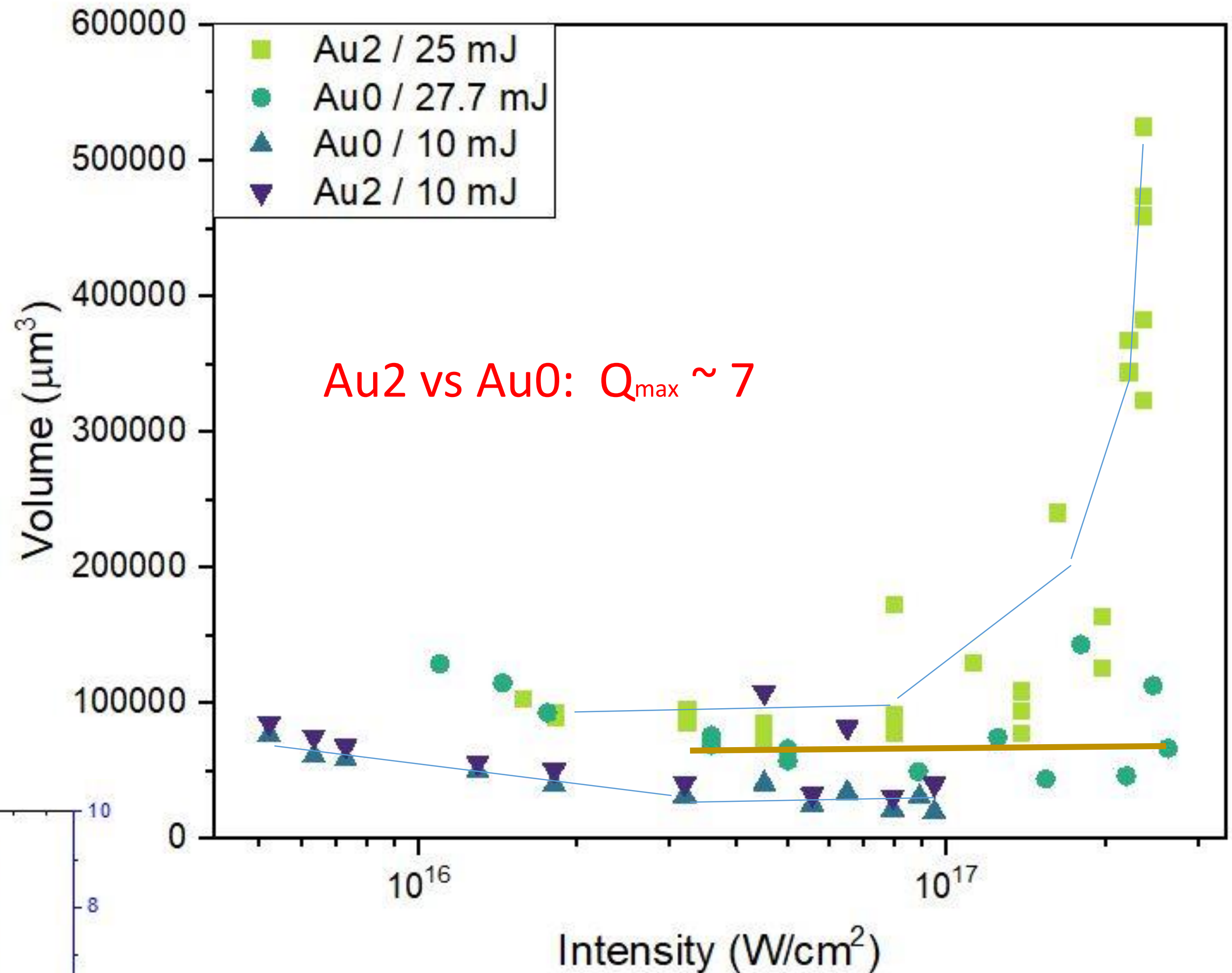


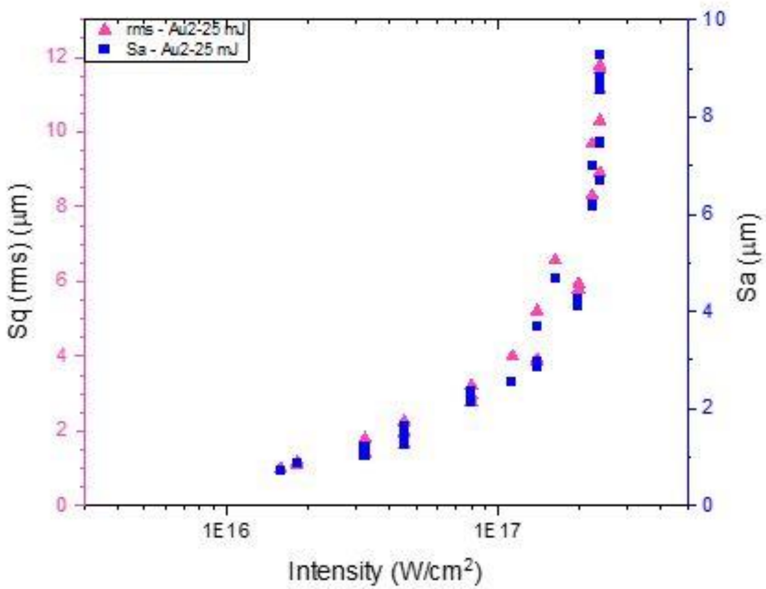


# CRATER VOLUME
# SURFACE ROUGHNESS

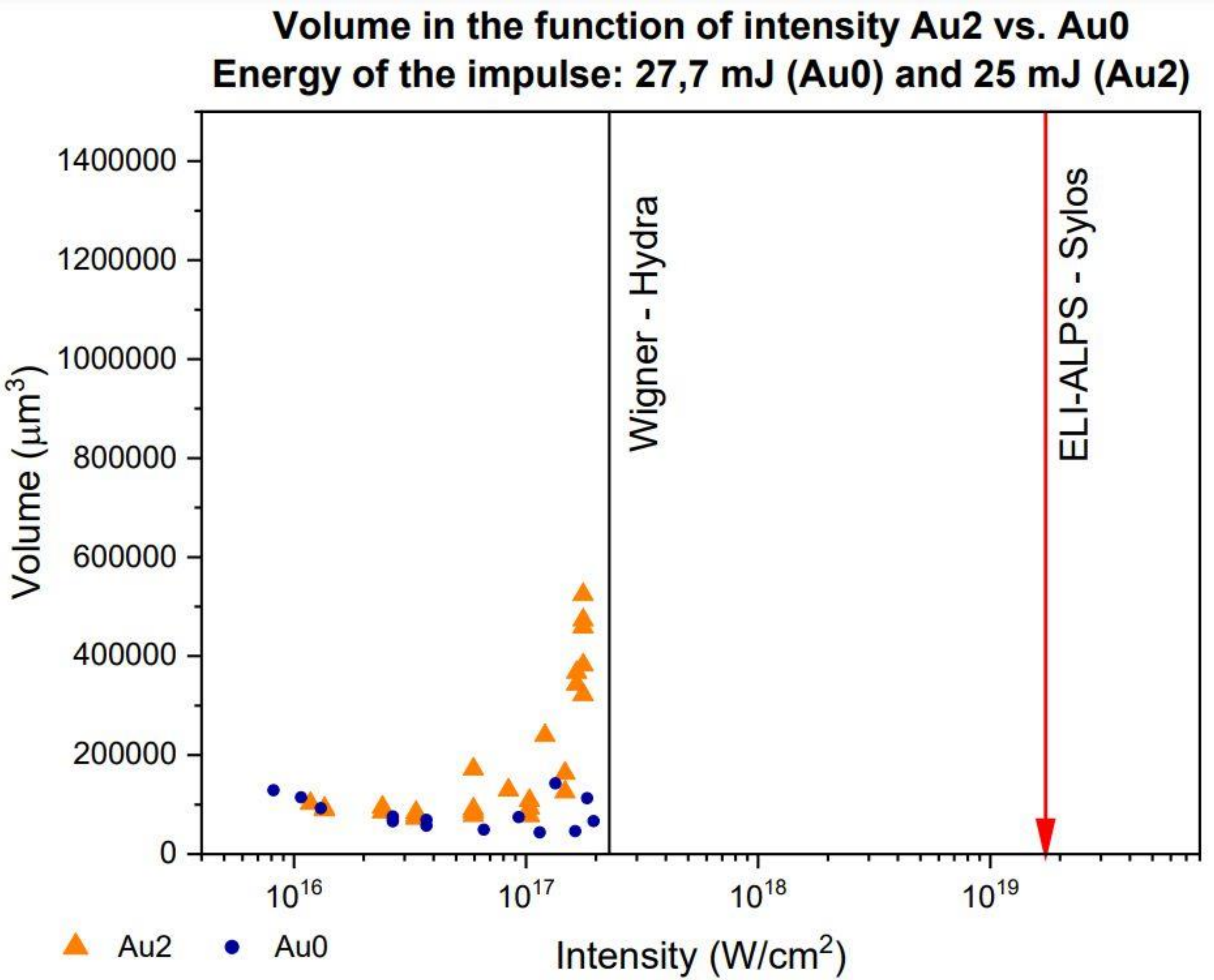

Volume in the function of intensity Au2 vs. Au0
Energy of the impulse: 27,7 mJ (Au0) and 25 mJ (Au2)
Volume (μm3)
1400000
1200000
1000000
800000
600000
400000
200000
0
Wigner - Hydra
ELI-ALPS - Sylos
10^16
10^17
10^18
10^19
Intensity (W/cm2)
Au2
Au0

# 2.Diagnozis :Raman scattering from the crater surface

arXiv2210.00619(2022),submitted to Advanced Optical Materials

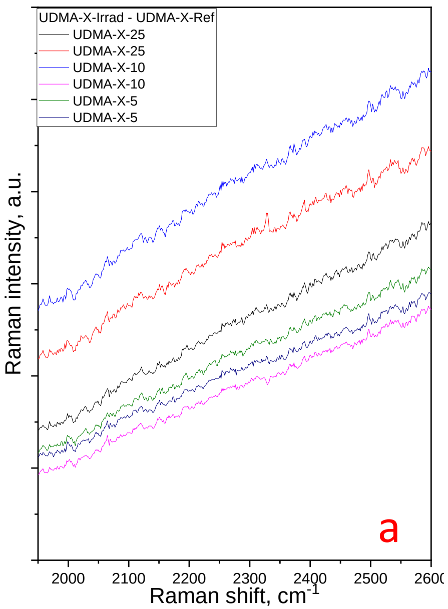


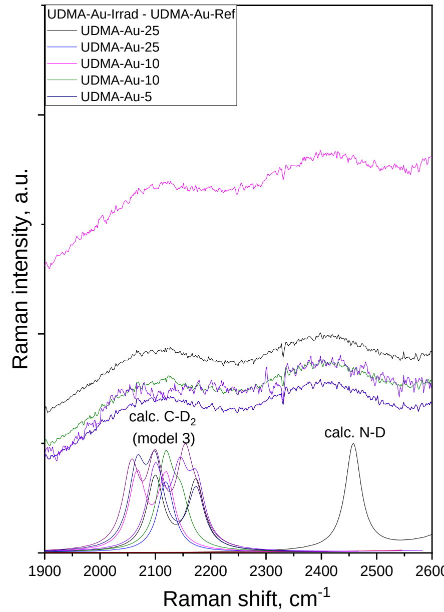


a: Au0

b: Au2

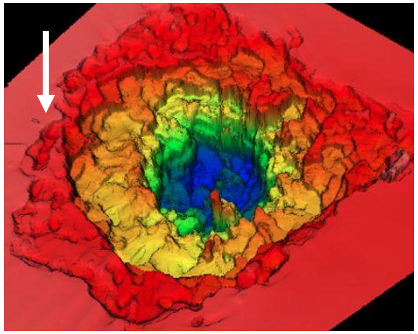

$I_{laser} > 10^{16}$ W/cm²

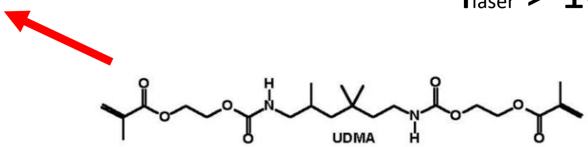


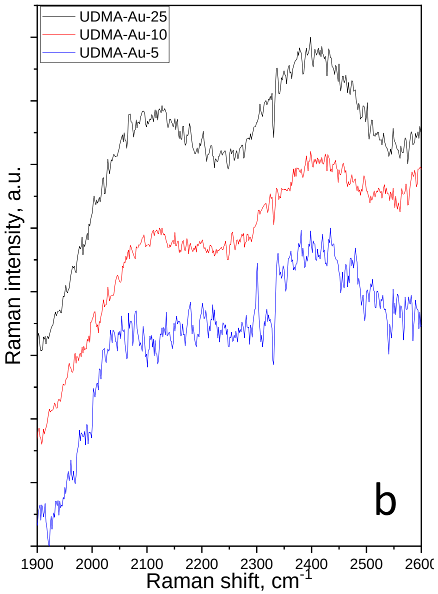


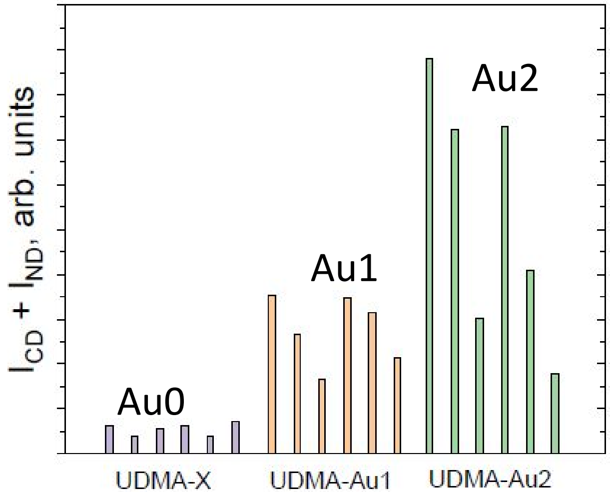


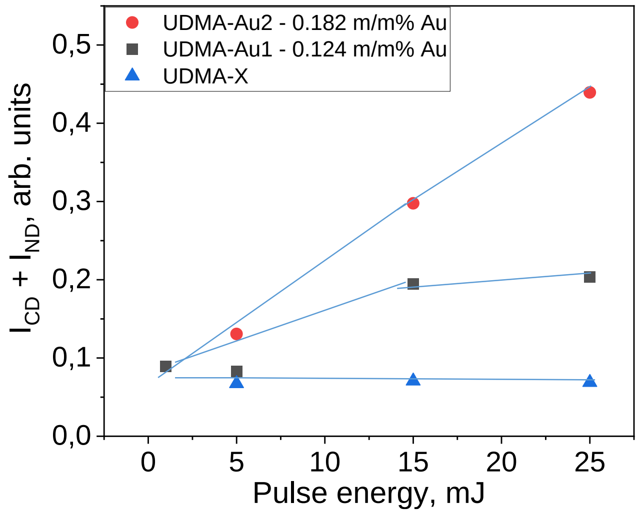

# 3.SOME RESULTS OF THE Hα AND Dα SPECTRAL LINES

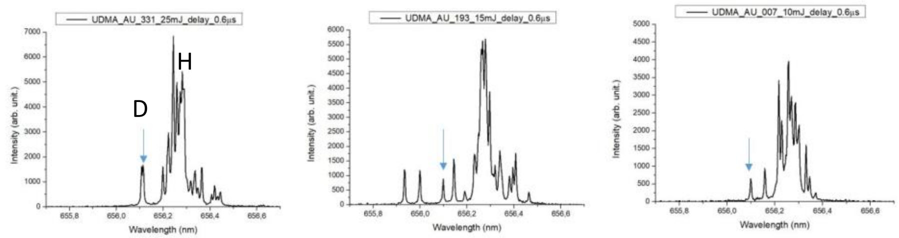


D/(2D+H): 10 +/- 0.9% 4.5 +/- 0.3% 4.2 +/- 0.4%

TYPICAL LIBS SPECTRA (at 3 laser pulse energies with and without Au nanoparticles)

No deuterium line

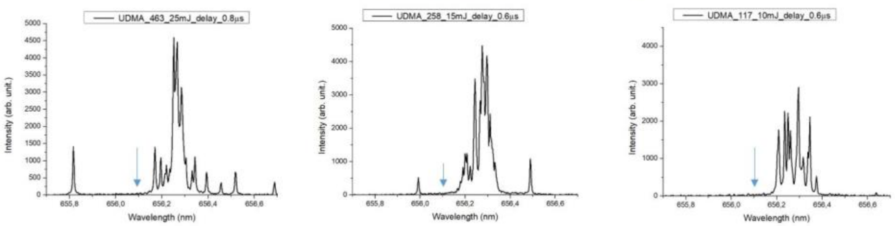


?

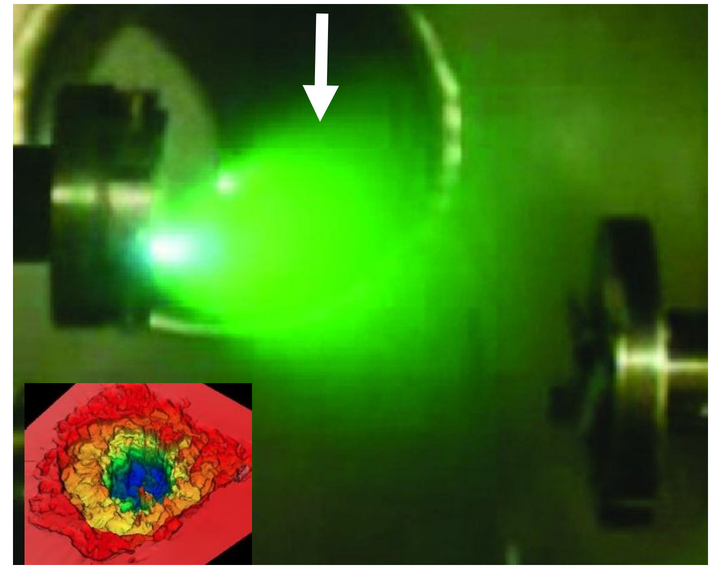

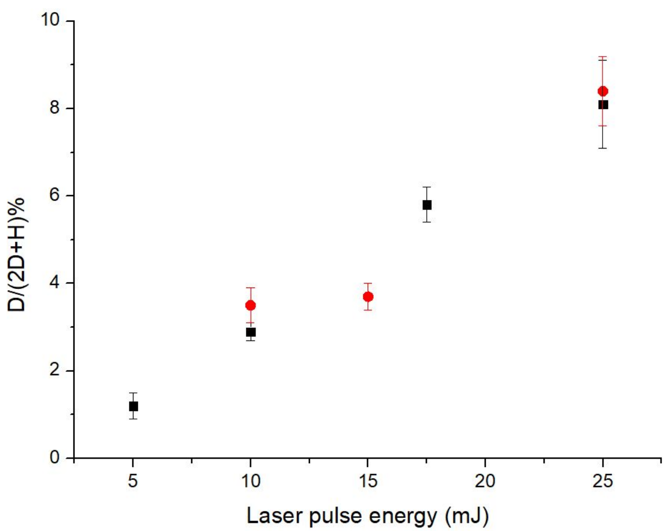


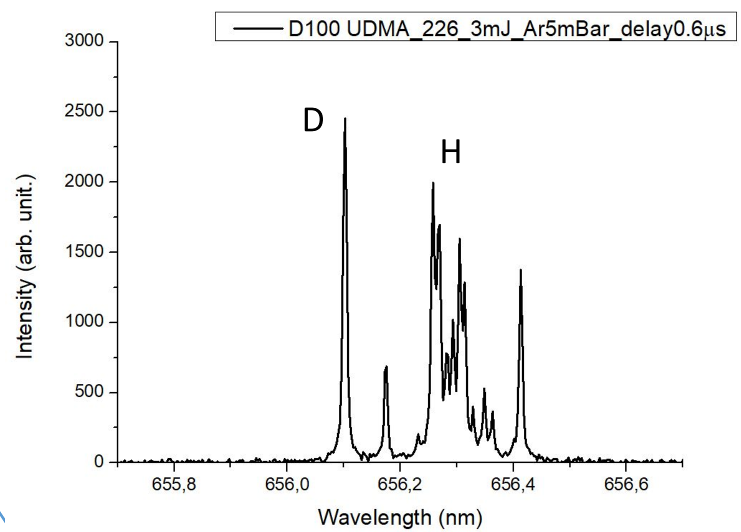


Deuterated (30%) sample

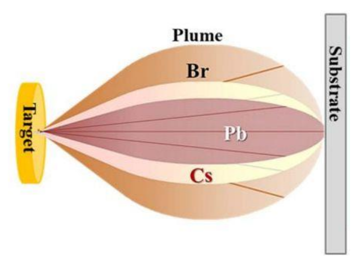


2D+H The total number of H atoms before the transmutation process

Number of D atoms in the case of 25mJ laser pulses : ~$0.4 \times 10^{14}$

# CRATER – LIBS CORRELATION

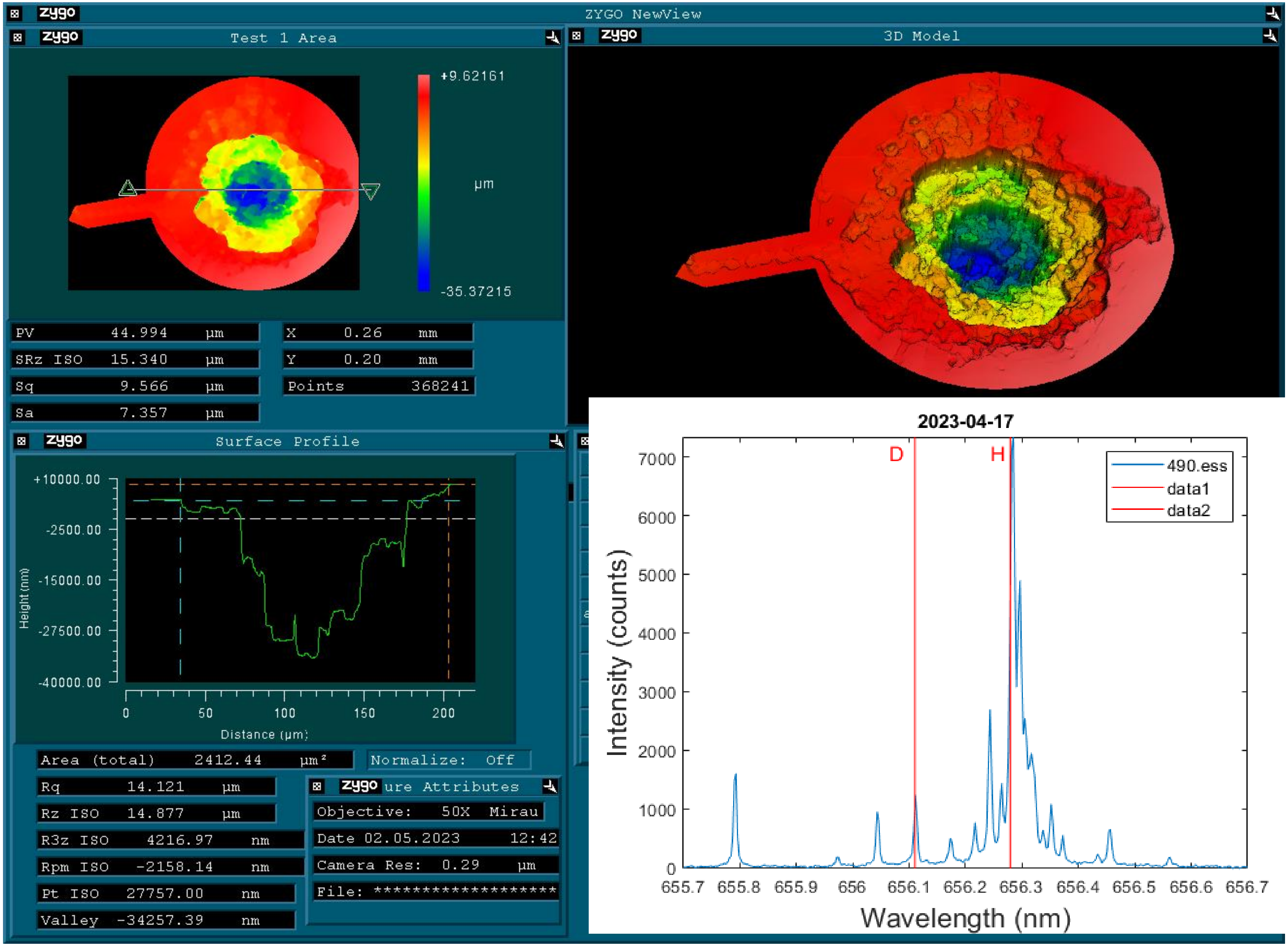

# IN WORK BUT NOT YET CONCLUDING TECHNIQUES:

1. Atomic optical spectroscopy,
2. Mass spectrometry.
3. Nuclear detection techniques.

1

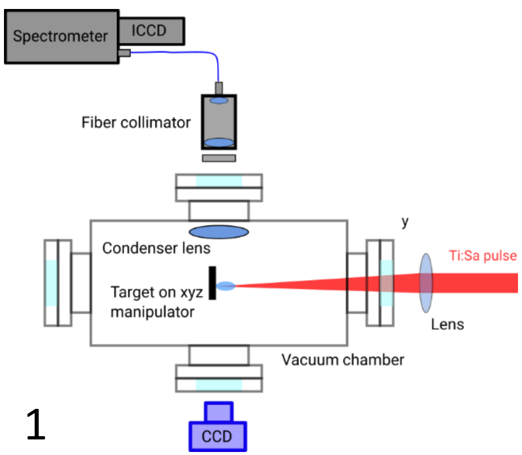


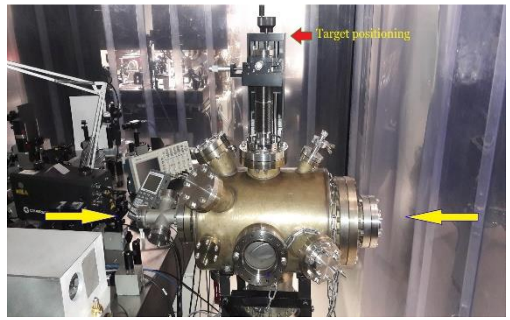


3: CR39 film, 1 laser shot

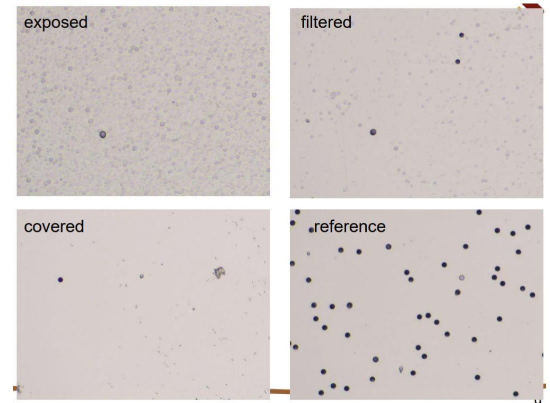


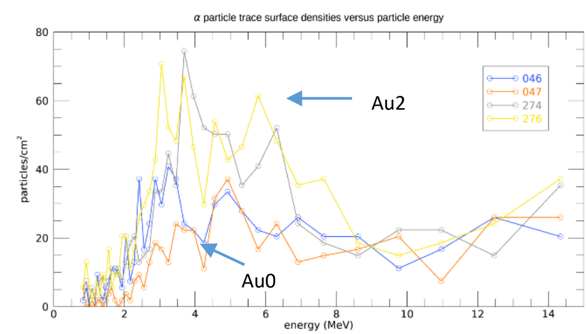


2

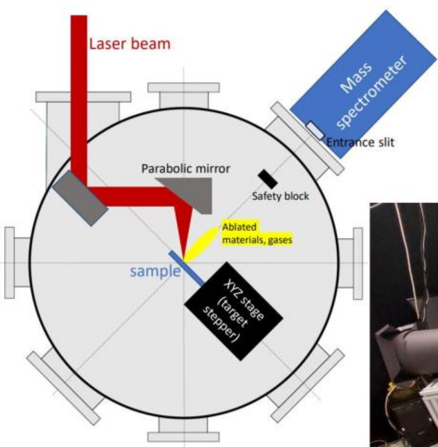


Experimental arrangement

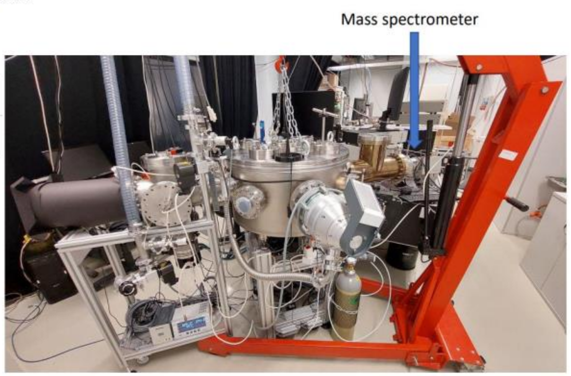


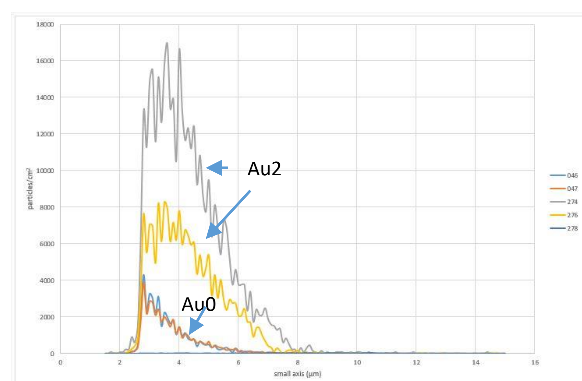


Boron nitride seeded samples

# 4. DIREKT NUCLEAR PROOF? (in vacuum?)

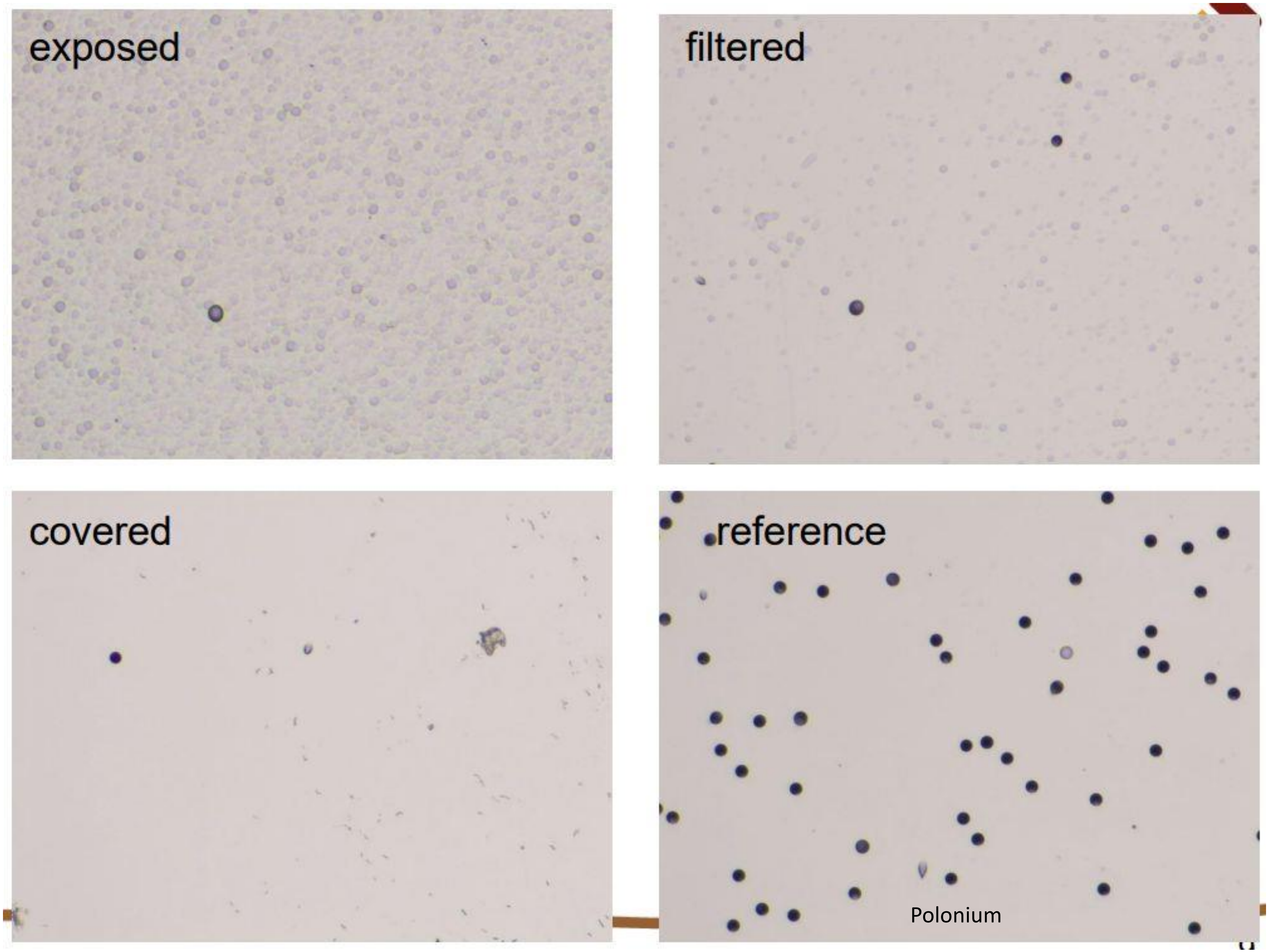


SYLOS LASER (up to $10^{19}$ W/cm², $10^{10}$ contrast, single shots
and later up to the
2PW (?) LASER ( 1Hz, ~10fs, 30 J, $10^{12}$ contrast

# Comparing modern approaches

**How close are we to "space plane" fusion in both the figurative and literal sense? How will we power the real future space planes that can travel across the solar system?**

**4,000 years**

**100 years**


**Recap:**

- $\mu CF$ opened the door to considering fusion processes outside the thermal regime
- pB laser driven fusion remains an essential technological exploration towards table-top fusion
- Plasmonic fusion satisfies all the requirements of truly table-top fusion:
    - Femto-attosecond high contrast laser pulse
    - Aneutronic
    - Different nuclear fuels can be attempted
    - Today exploring processes with scalable commercial laser technology
    - Transferable to ELI-Alps laser for large scale energy production

**!**

From: Jan Rafelski

# SUMMARY:

-Localized plasmons (LSPP) differ from the propagating ones with positive consequences.
-Properties are shape and material dependent (Au and Ag resonances in the visible spectrum)
-At high laser intensities no plasma mirror effect.
-Nanoparticles are effective at high laser intensities. Field amplification (hot spots).
Optimal lifetime for femtosecond lasers (e.g. Ti:Sa, 800nm)
Simplified geometry (one or two biams)
Screening (near field and ponderomotive effect)
Correlated momentum transfer
-Energy production (crater volume up to 8 times larger with Au nanorods) and $H \longrightarrow D$ transmutation (fusion) as the explanation, indicated by Raman scattering on the C-D and N-D vibrations and LIBS $D^{\alpha}$ latomic spectral line.
-Supportive modelling results.
-Still several open questions.

# AND OUR GOAL IS:

To strengthen these results and reach further ones, based on LSPP properties with the intention to

- -drive for efficient nanoplasmonic aneutronic fusion reactions,
- -and this way scale down the size and costs of future laser based nuclear fusion facilities;
- -find solutions at the lowest possible optimal laser pulse energies;

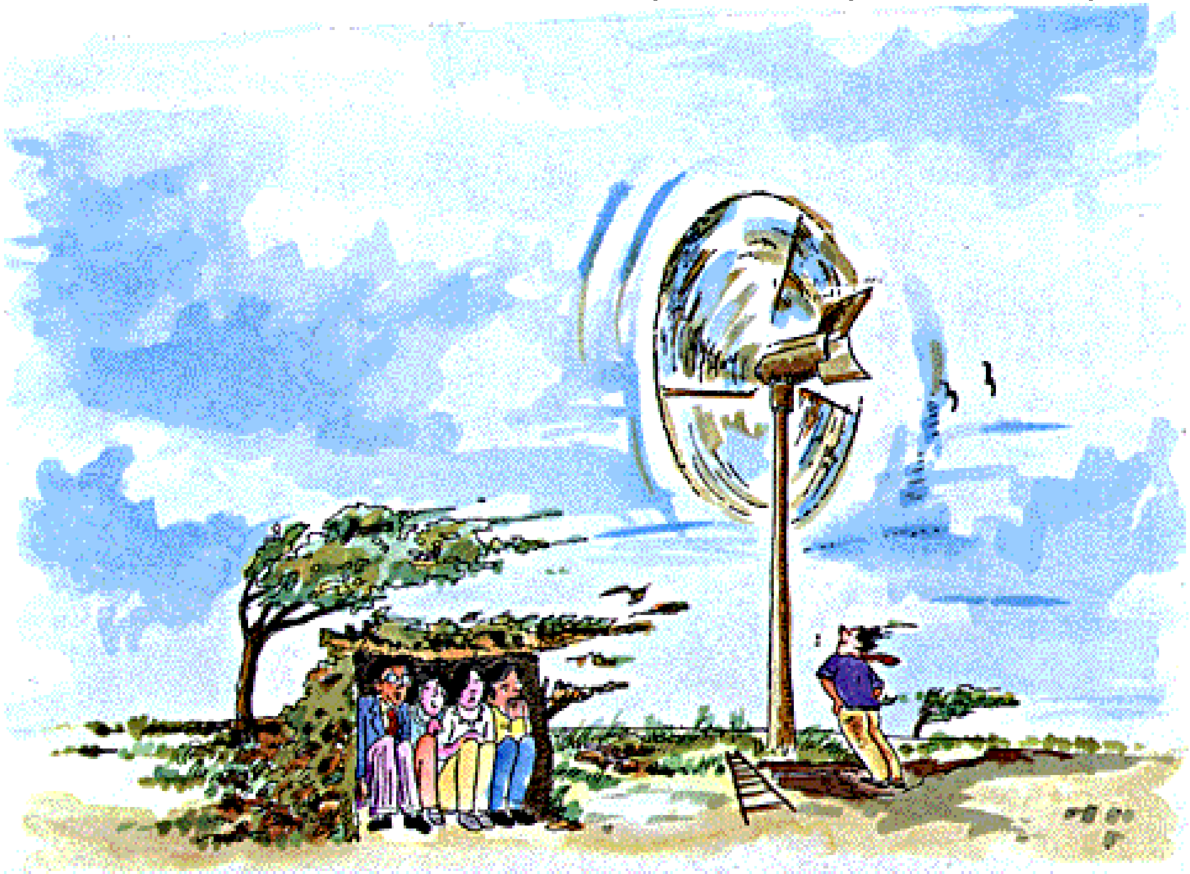

When the winds of changes are blowing some build shelters, but some others build wind turbines

European Commission

# Technology Readiness Levels

**TRL 0: Idea**. Unproven concept, no testing has been performed.

**TRL 1: Basic research.** Principles postulated and observed but no experimental proof available.

**TRL 2: Technology formulation**. Concept and application have been formulated.

**TRL 3: Applied research**. First laboratory tests completed; proof of concept.

**TRL 4: Small scale prototype** built in a laboratory environment ("ugly" prototype).

**TRL 5: Large scale prototype** tested in intended environment.

**TRL 6: Prototype system** tested in intended environment close to expected performance.

**TRL 7: Demonstration system** operating in operational environment at pre-commercial scale.

**TRL 8: First of a kind commercial system**. Manufacturing issues solved.

**TRL 9: Full commercial application**, technology available for consumers.

# THANKS FOR YOUR ATTENTION!